

Copyright Warning & Restrictions

The copyright law of the United States (Title 17, United States Code) governs the making of photocopies or other reproductions of copyrighted material.

Under certain conditions specified in the law, libraries and archives are authorized to furnish a photocopy or other reproduction. One of these specified conditions is that the photocopy or reproduction is not to be “used for any purpose other than private study, scholarship, or research.” If a user makes a request for, or later uses, a photocopy or reproduction for purposes in excess of “fair use” that user may be liable for copyright infringement,

This institution reserves the right to refuse to accept a copying order if, in its judgment, fulfillment of the order would involve violation of copyright law.

Please Note: The author retains the copyright while the New Jersey Institute of Technology reserves the right to distribute this thesis or dissertation

Printing note: If you do not wish to print this page, then select “Pages from: first page # to: last page #” on the print dialog screen

The Van Houten library has removed some of the personal information and all signatures from the approval page and biographical sketches of theses and dissertations in order to protect the identity of NJIT graduates and faculty.

ABSTRACT

AN AUTOMATED APPROACH FOR COMPARATIVE ANALYSIS OF QT INTERVAL AND HEART RATE VARIABILITY

by

Taral Oza

Cardiovascular disease is the primary cause of death in the adult population. Half of these cardiac deaths occur as sudden death. Some of the parameters from the surface ECG recording (a noninvasive technique) carry important information and have special significance in research, as they are good indicators of diseases leading to heart attacks, sudden cardiac death and other similar cardiac problems. Measurement of QT interval variability and heart rate variability are two such parameters, which has received much attention of researchers.

An algorithm has been developed to measure and compare the two significant parameters, the QT interval variability and the heart rate variability. Agilent's VEE Pro[®] 6.0 software is used as graphical tool to implement signal processing operations. This algorithm detects peaks from the ECG including the Q, R, S, T and the end of the T wave. These peaks are use to calculate both, the heart rate variability and QT interval variability. The algorithms have been tested on normal and diseased patient data from the standard MIT ECG library to prove the accuracy and reproducibility of the system. Observations about the amount of influence of the autonomic nervous system on the heart rate variability and QT interval variability have been carried out. Results indicate that behavior of the autonomic nervous system is different for normal patient and diseased patients. Diagnosis of Coronary Artery Disease is done very reliably using this system.

**AN AUTOMATED APPROACH FOR COMPARATIVE ANALYSIS OF
QT INTERVAL AND HEART RATE VARIABILITY**

by

Taral Oza

**A Thesis
Submitted to the Faculty of
New Jersey Institute of Technology
in Partial Fulfillment of the Requirements for the Degree of
Master of Science in Biomedical Engineering**

Department of Biomedical Engineering

January 2001

Blank Page

APPROVAL PAGE

**AN AUTOMATED APPROACH FOR COMPARATIVE ANALYSIS OF
QT INTERVAL AND HEART RATE VARIABILITY**

Taral Oza

Dr. Ronald H. Rockland, Thesis Advisor Date
Assistant Professor of Engineering Technology and Biomedical Engineering, NJIT

Dr. Stanley S. Reisman, Committee Member Date
Professor of Biomedical Engineering, NJIT

Dr. Richard Foulds, Committee Member Date
Associate Professor of Biomedical Engineering, NJIT

BIOGRAPHICAL SKETCH

Author: Taral Oza

Degree: Master of Science in Biomedical Engineering

Place of Birth: Botad, Gujarat, India

Undergraduate and Graduate Education:

- Master of Science in Biomedical Engineering
New Jersey Institute of Technology, Newark, NJ 2001
- Bachelor of Engineering in Instrumentation and Control
Dharmsinh Desai Institute of Technology, Nadiad, Gujarat, India 1998

Major: Biomedical Engineering

This thesis is dedicated to my elder brother
Ketul Trivedi for his immense support all through my career.

ACKNOWLEDGEMENT

Any fulfillment is a mélange of executions by more than one. And while only one enjoys the center, the perimeter must not be disregarded. In my opinion, it is they who actually deserve credit for the job accomplished. Hence, while summing up my research thesis with this concise report, I would like to express my gratitude to all those who have helped me reach so far.

My first and foremost gratitude is to Dr. Ronald H. Rockland, who, since day one, has completely guided me in all technical matters. As my research guide, he provided me with more knowledge than I have ever consumed in so short a span. He patiently spelled out all new concepts to me, and helped me assimilate them correctly. He was an overall inspiration to me throughout my tenure at NJIT, and will be for the years to come. I am truly indebted to him.

Thanks are in order to Dr. David Kristol, Dr. Richard Foulds, Dr. Stanley Reisman and Dr. Peter Engler, whose contributions in this attainment are gratefully acknowledged. Each of them assisted me in learning the most difficult of topics, and also helped me with numerous other small and large matters.

Also, numerous thanks to everyone in the Biomedical Engineering department. I could not possibly miss expressing my appreciation for Mr. Dhawal Desai, Mr. Darnell Simon, and Dr. Bruno. They were not only excellent friends and compassionate individuals, but also kind enough to participate in my research.

I would like to thank Dr. Ronald Kane, Ms. Gayle Katz and other staff members of the Graduate Studies and International Student Offices. All of you, I am truly thankful for all that you did for me.

Finally, my gratitude to God, my parents and my sister, my cousins and all friends, who have encouraged me all through. With Your Grace, the impossible's been true till date.

"Whatever a man's achievements, they are unquestionably a product of affectionate people who nurtured his aspirations. Those who hold one in high esteem, who encourage him in moments of confusion and despair, who support his self-confidence by sharing his dreams, and who urge him into the future by their expressed faith in his capacities, are surely the agents of his unfolding"

Harry Levinson

Harvard Business School

TABLE OF CONTENTS

Chapter	Page
1 INTRODUCTION.....	1
1.1 The Heart – A Synopsis.....	1
1.2 Electrophysiology.....	2
1.3 Interval Measurement – An Overview.....	7
1.3.1 QT Interval.....	8
1.3.2 Heart Rate Variability.....	9
1.4 The Autonomic Nervous System.....	10
2 RESOURCES.....	12
2.1 Using VEE.....	13
2.2 Acquisition of Data.....	16
2.2.1 MIT-BIH Database.....	16
2.2.2 Method to View and Convert Records.....	18
2.3 Selection of Samples.....	19
3 THE ALGORITHM.....	23
3.1 Getting the Proper Inputs.....	25
3.2 Filtering.....	25
3.3 R Wave Detection.....	27
3.3.1 Adaptive Threshold.....	28
3.3.2 Peak Detection from Derivative Signal.....	29
3.3.3 Find Zero Crossing Points.....	30

TABLE OF CONTENTS
(Continued)

Chapter	Page
3.4 Q Wave Detection.....	31
3.4.1 Defining Windows.....	32
3.4.2 Detecting Q Peaks.....	32
3.4.3 Detecting Q Wave Beginning.....	32
3.5 T Wave Operations.....	33
3.5.1 Separating Windows.....	33
3.5.2 Detection of S Wave.....	35
3.5.3 Detection of T Peaks.....	35
3.5.4 End Of T Wave Detection.....	36
3.6 QT Interval Measurements.....	36
3.7 Obtaining IIBI and Power Spectrum.....	38
4 RESULTS AND CONCLUSION.....	42
4.1 R Wave Validation.....	42
4.2 Q and T Wave Results.....	43
4.3 Comparative Analysis.....	45
4.4 Discussions and Future Work.....	47
APPENDIX A SCREENSHOTS AND OTHER RESULTS.....	49
APPENDIX B AN EXAMPLE OF PROGRAM DOCUMENTATION.....	54
REFERENCES.....	58

LIST OF TABLES

Table	Page
1. List of samples from MIT-BIH arrhythmia database.....	20
2. Samples from european ST-T database.....	21
3. Samples from normal sinus rhythm database.....	22
4. Validation of R wave detection algorithm.....	43
5. T-test results comparing each parameter between normal and CAD patients.....	45
6. T-test results for parameter comparison for CAD patients.....	45
7. T-test results for parameter comparison for normal patients.....	45
8. Results for number of total beats analyzed	53

LIST OF FIGURES

Figure	Page
1. Cross sectional view of the heart.....	1
2. Steps of excitation in the heart.....	2
3. The electrical pathway of impulse through the heart.....	3
4. Amplitudes and time intervals in the ECG.....	4
5. Lead arrangement.....	6
6. Intervals in the ECG.....	7
7. Rhythms of the ECG.....	11
8. Panel view in VEE.....	15
9. Main view in VEE.....	15
10. Functional blocks in the program.....	24
11. Filtering process.....	26
12. Peak detection using the first derivative of the signal.....	30
13. R peaks detection results.....	31
14. R peaks detected in a noisy piece of signal.....	31
15. S wave, T peaks and end of T wave results.....	36
16. Sample IIBI plot.....	38
17. Sample power spectrum from a healthy patient.....	40
18. Sample power spectrum for QTc.....	40
19. Sample power spectrum for QTcc.....	41
20. Q wave results.....	44
21. Screenshot of input module.....	49

LIST OF FIGURES
(Continued)

Figure	Page
22. Screenshot of filtering module.....	50
23. Screenshot of threshold calculation routine.....	51
24. R peak detection routine.....	52

CHAPTER 1

INTRODUCTION

1.1 The Heart – A Synopsis

The use of engineering methods, the development of instrumentation and use of computers for diagnosis has contributed substantially to progress made in recent years in helping reduce the number of death from heart diseases. One such advancement in the diagnosis of heart disease is non-invasive measurement of the heart's electrical activity.

The heart is a hollow muscular organ lying in the center of the chest (thorax) contains four chambers; right atrium, right ventricle, left atrium and left ventricle. Each of the four chambers of the heart is different from the others because of its functions. The heart normally behaves as a pump used to force the blood through the cardiovascular system with the function of providing oxygen to the whole body and eliminating the body of metabolic wastes, like carbon dioxide.

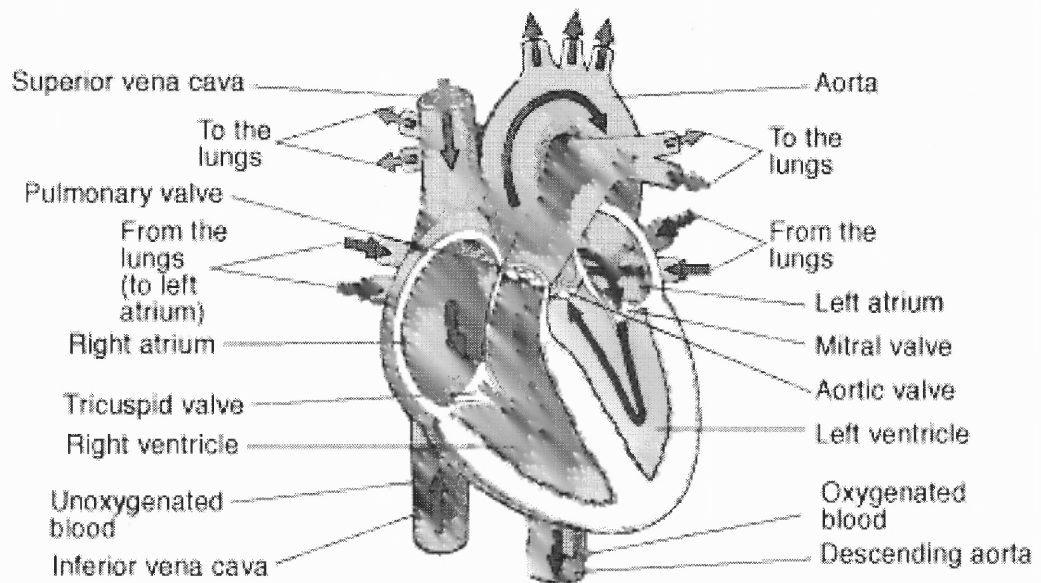


Figure 1: Cross sectional view of the heart [1].

1.2 Electrophysiology

Unlike most other muscle innervations, excitation of the heart does not proceed directly from the central nervous system but is initiated in the sinoatrial (SA) node (also known as the pacemaker of the heart). The SA node is a collection of excitable cells. The SA node generates an impulse of excitation that spreads across the left and right atrium causing the atria to contract. A short time later, it simulates the atrioventricular (AV) node initiating the impulse into the ventricles. From the AV node the impulse continues down through the bundle of His followed by special conducting fibers called the Purkinje Fibers on either side of the ventricle causing simultaneous contraction throughout the ventricle [1]. The contraction resulting in the myocardium supplies the force to pump the blood into the circulatory system. Hence, the frequency of SA node impulses mainly controls the heart rate. A detail discussion on the electrical events of the heart is presented in the following sections.

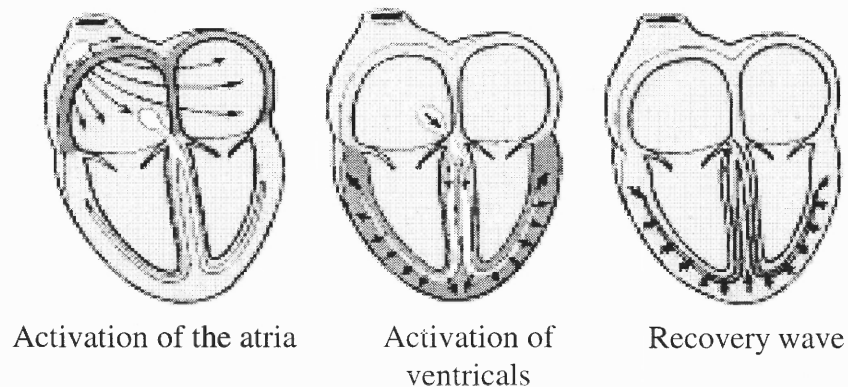


Figure 2: Steps of excitation in the heart [1].

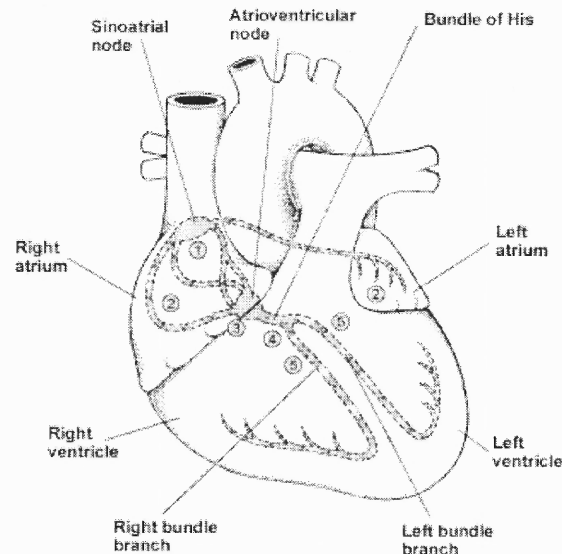


Figure 3: The electrical pathway of impulse through the heart [1].

In figure 3, an electrical impulse generated by the SA node (1) flows over the right and left atria (2) causing them to contract. When the electrical impulse reaches the AV node (3), it is delayed slightly. The impulse then travels down the bundle of His (4), which divides into the right bundle branch for the right ventricle (5) and the left bundle branch for the left ventricle (5). The impulse then spreads over the ventricles, making them contract.

An electrocardiogram (ECG or EKG) is a measure of the electrical events within the heart or a display of the time-variant voltages produced by the myocardium during the cardiac cycle. The ECG is used clinically to diagnose various diseases and to assess cardiac health. Since the ECG is measured with respect to time, it also serves as a timing reference for other measurements. In a typical ECG, alphabetical designations (P, Q, R,

S, and T) have been assigned to each of the prominent features. These can be identified with events related to the action potential propagation pattern.

The P, QRS and T waves reflect the rhythmic electrical depolarization and repolarization of the myocardium associated with the contractions of the atria and ventricles. The P wave represents depolarization of the atrial musculature. The QRS complex is the combined result of the repolarization of the atria and the depolarization of ventricles that occurs almost simultaneously. The T wave represents ventricular repolarization. Typical amplitude of each wave is listed below [2].

- P wave – 0.25 mV
- R wave – 1.6 mV
- Q wave – 25% of R wave
- T wave – 0.1 to 0.5 mV

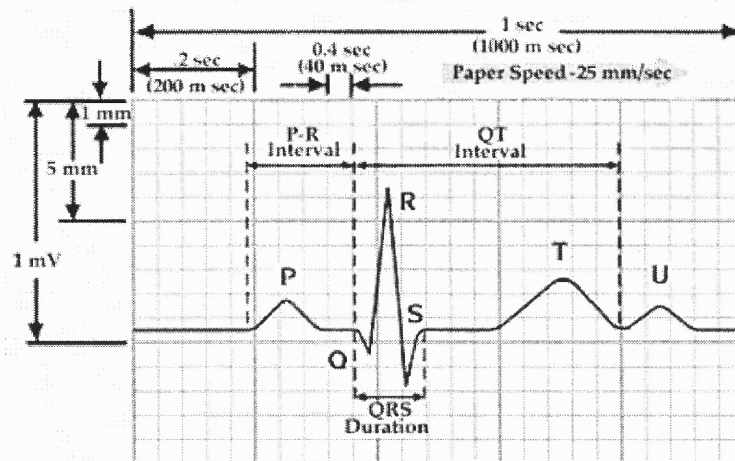


Figure 4: Amplitudes and time intervals in the ECG [3].

The shape and polarity of each of these features vary with the location of the measuring electrodes with respect to the heart. To measure an ECG, a number of

electrodes are affixed on the skin of the person's arms, legs, and chest. These electrodes measure the flow and direction of electric currents in the heart during each heartbeat. The electrodes are connected to a machine, through wires or wireless transmission, which produces a tracing for each electrode. A particular group of electrodes, when they are connected with recording amplifiers, represents a particular "view" of the heart's electrical patterns; these views are called leads. The 12 standard leads used most frequently are shown in the following diagram. The three bipolar limb lead selections, first introduced by Einthoven, are derived from electrodes placed on the limbs [2].

- Lead I : Left Arm and Right Arm
- Lead II : Left Leg and Right Arm
- Lead III: Left Leg and Left Arm

Generally the bipolar leads are arranged such that the R wave of a normal heart is positive. The other leads can be divided into unipolar limb leads and unipolar chest leads. Unipolar limb leads include aVR, aVL and aVF. Six unipolar chest leads are designated as V1 to V6.

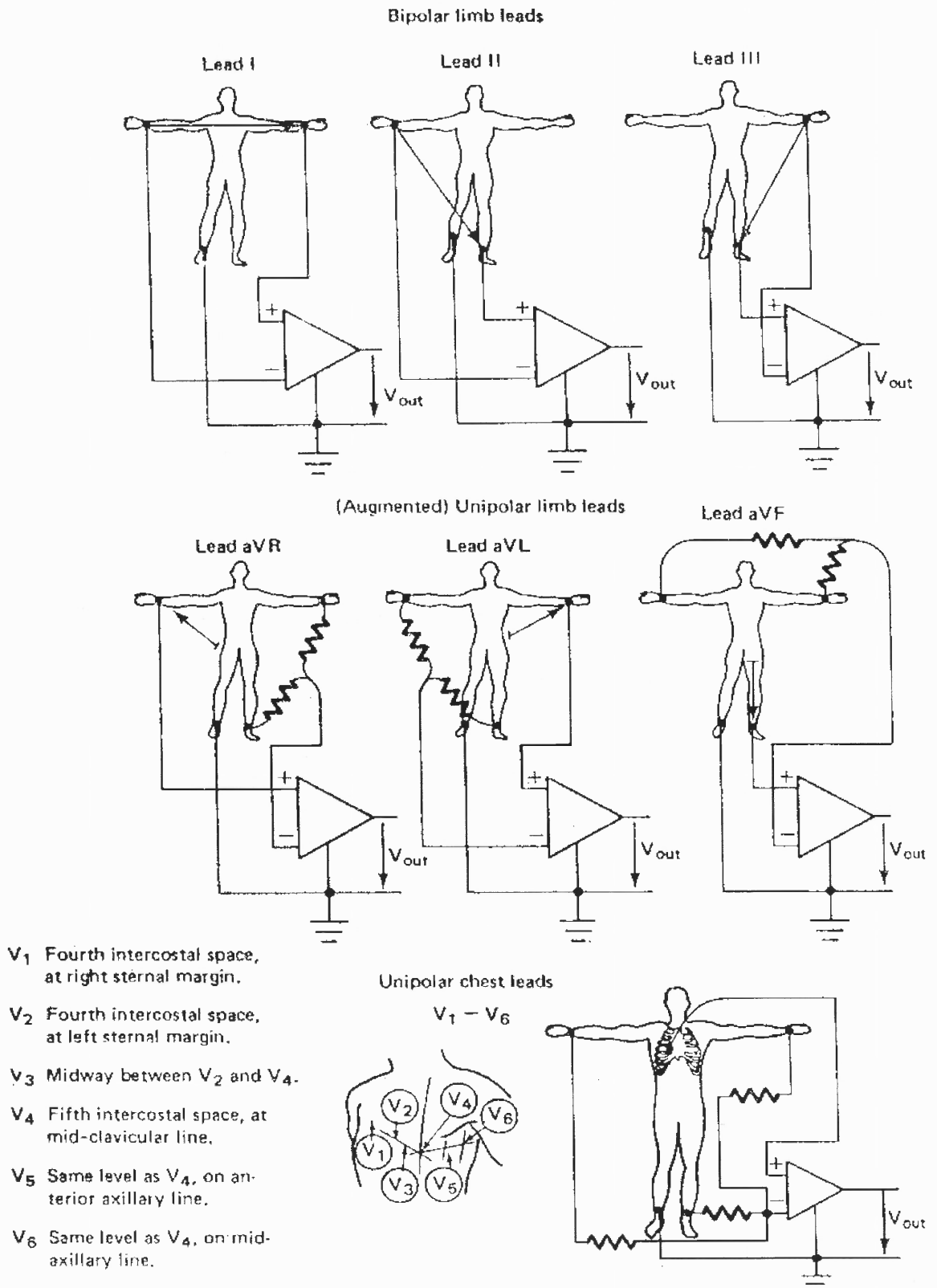


Figure 5: Lead arrangement [2].

1.3 Interval Measurement – An Overview

As each ECG interval is related to some physiological activity, each interval gives vital information about the patient's heart. The accepted normal interval durations are as follows [2]:

- P-R interval – 0.12 to 0.2 second
- Q-T interval – 0.35 to 0.44 second
- S-T segment – 0.05 to 0.15 second
- P wave duration – 0.11 seconds
- QRS duration – 0.09 seconds

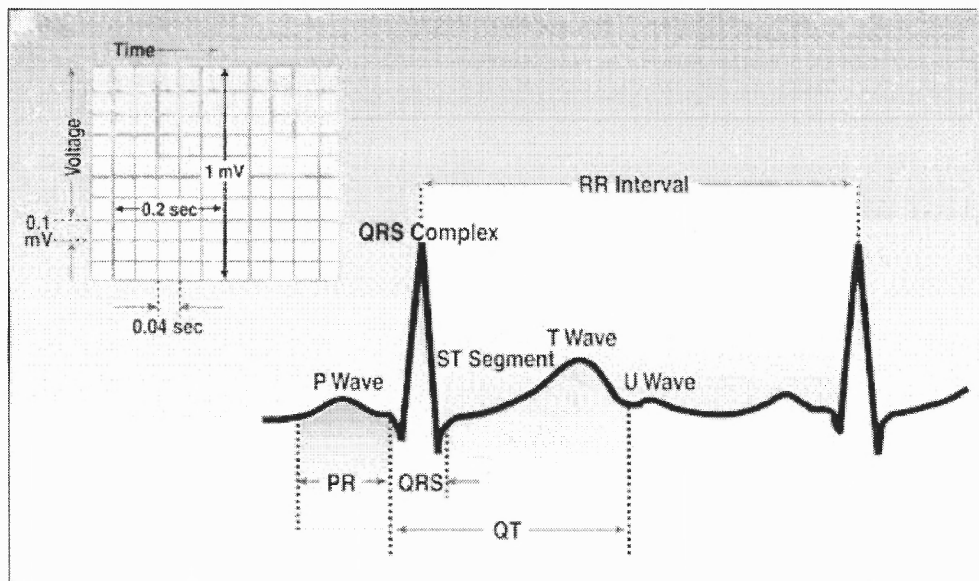


Figure 6: Intervals in the ECG [3].

The P-Q interval represents the time delay caused by the AV node. If the P-R interval is greater than 0.2 second, blockage of the AV node can be suggested. The R-R interval is used to measure the person's heart rate.

1.3.1 QT Interval

Cardiovascular diseases have engaged researchers to develop new methods to diagnose the onset of the diseases that can lead to mortality. Measurement of beat-to-beat QT interval is also considered for various such research studies. Alagra *et al* [4] hypothesize that rapid changes of the QT interval can lead to life threatening situations. The measurement of QT interval has influence of heart rate changes while performing analysis on it. Hence, to obtain better results, QT interval is corrected by a formula called Bazett's formula ($QTc = QT/(RR)^{1/2}$) and a new parameter is called QTc (QT corrected) [5]. An abnormal QTc can be associated with serious ventricular arrhythmias, syncope and sudden cardiac death [5]. Also, increased risk of sudden cardiac death due to the QTc prolongation is independent of age, history of acute myocardial infarction, heart rate and drug usage [6].

Abnormal changes in the activity of the sympathetic nervous system can cause QTc prolongation and deterioration of an initial sinus rhythm into ventricular fibrillation [7]. The present research emphasis is to resolve some of the problems encountered in the QT interval analysis and to describe a new algorithm that is robust and reliable to analyze the QT interval on a beat-to-beat basis. Several methods exist for the measurement of the QT interval. Correct detection of the Q wave and the end of the T wave are required to accurately measure the QT interval and QT interval variability. Some QRS morphologies allow consistent detection of the Q wave and the end of the T wave whereas some continuously changing QRS morphologies can cause error in the accurate detection process.

1.3.2 Heart Rate Variability

The measurement of RR interval variability is called heart rate variability (HRV). Generally low heart rate variability predicts increased mortality. M. Malik, V. Batchvarov [8] accredited Hon and Lee [9] with first appreciating the clinical significance of HRV in 1965. The authors also mentioned Wolf [10] as the first to associate higher risk of post infarction mortality with reduced HRV in 1977 and Akselrod [11] introduced power spectral analysis of heart rate fluctuations to quantitatively evaluate beat-to-beat cardiovascular control.

The time domain method is one method to measure HRV. In this method, the intervals between successive normal QRS complexes are determined. The time interval between these successive QRS complexes allows measurement of instantaneous heart rate. Various statistical results, such as the mean of the RR interval and the mean heart rate can be obtained by this method.

More complex statistical time domain measurement has also been used in various studies. The variable SDNN is the standard deviation of the interval between two successive normal QRS complexes (called Normal-to-Normal (NN) intervals). These methods allow comparison of HRV during various activities like pace breathing, tilt, valsalva maneuver, phenylephrine infusion, rest, sleep and so on. Generally total variance of HRV increases with the length of the analyzed recording [8]. Other short term variations can be measured using parameters like the standard deviation of the average NN intervals (SDANN) and the square root of the mean squared difference of successive NN intervals (RMSSD).

Various frequency domain methods are also useful for analysis of cardiac signal. One such method is to construct the interbeat interval (IBI) signal and power spectral calculations. Frequency domain measurements indicate the autonomic nervous system activities. Detail explanation about frequency domain methods is described later in this document.

1.4 The Autonomic Nervous System

The part of the nervous system that regulates the heart rate is the autonomic nervous system, which consists of the sympathetic and parasympathetic nervous systems. The sympathetic system speeds up the heart rate; the parasympathetic system slows it down. Due to predominant parasympathetic activity during the resting state, the normal heart rate is below 100 beats/minute. The sympathetic system supplies the heart with a network of nerves, the sympathetic plexus, while the parasympathetic system supplies the heart through a single nerve, the vagus nerve. Both the parasympathetic and the sympathetic nervous systems terminate at the following locations: SA node, the conduction system, atrial and ventricular myocardium and coronary vessels but the parasympathetic nervous system also extends up to the AV node [1].

The reciprocal activity of the sympathetic and parasympathetic nervous systems causes fluctuations in the heart rate. However, under certain conditions only one division of the nervous system can have a significant effect on the heart rate.

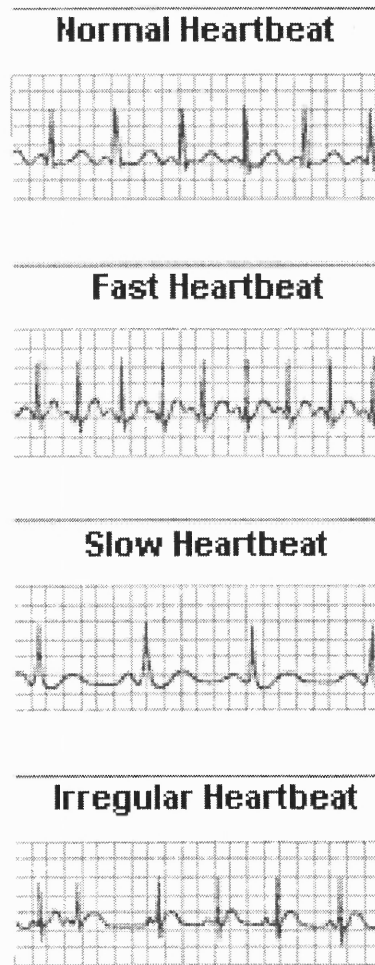


Figure 7: Rhythms of the ECG [1].

The normal heart rate at rest is usually between 60 and 100 beats per minute. However, much lower rates may be normal in adults, particularly those who are physically fit. The heart rate responds not only to exercise and inactivity but also to stimuli such as pain and anger. Tachycardia and bradycardia are two cases of abnormal heart rate. In tachycardia the heart rate is above the normal range for a particular person, whereas in bradycardia the heart rate is abnormally low. Abnormal rhythm of the heartbeats, called arrhythmia, is generally caused by the electrical impulses traveling in abnormal pathways.

CHAPTER 2

RESOURCES

The software used to implement the analysis process in this thesis is Agilent's VEE Pro[®] 6.0. This software is a graphical tool available to implement mathematical and logical operations. Inclusion of Matlab functions greatly enhance the usability of VEE Pro[®] for signal processing applications. The applications are created by placing graphical objects (blocks) on the working area and wiring them together with lines. This graphical view itself is the program. There is no need to perform any cryptic and error-prone steps like preprocessing, compiling, or linking. The entire program is made up of 'blocks' and looks like a 'block diagram'. There are two views in a VEE program. One is 'Panel View' and the other is the 'Main View'. The panel view is generally used to display final results and to create a user interface containing a navigation panel, command buttons, menu options, etc. The main view will show each component of the program. When the program (or 'block diagram') is ready, it can run just by pressing the 'Run' button.

Features like Program Explorer, Profiler, Function & Object Browser, etc. allows the user to manage variables and to measure the time taken by the program to produce results. Strong debugging features makes it easy for the development of complicated programs.

The sample data sets used in this thesis to validate the algorithms are taken from the MIT-BIH database. The method used to obtain data from the samples of the MIT-BIH database is described later in this chapter.

2.1 Using VEE

A simple example is discussed in this report to give some idea about the flexibility, convenience and efficiency of programming using VEE. The program below is a simple routine to detect the zero crossing from an array of numbers with size n , generated randomly with the condition that it should cross the zero line at least once. The purpose of the program is to find the point where the signal is crossing the zero line.

Following is the pseudo code for the routine:

1. *For $n=1$ to $n<m$, increase n by step of 1;*
2. *If $(A[n]*A[n-1])\leq 0$, that point indicates zero crossing. Due to discrete sampling, the signal may cross the zero line between two samples. This criteria ensures that zero crossing.*
3. *Compare absolute of $(A[n]-0)$ with absolute of $(A[n-1]-0)$ and find the smaller one to find the point close to the zero line.*
4. *Result will be $A[n]$, if $A[n]$ is smaller; otherwise, it's $A[n-1]$.*

where n is the index of the array element, m is the total size of the array and $A[n]$ is n th element of array A .

The Main view in figure 9 contains the block diagram of the program. To implement this routine in VEE, an array of twenty elements has been generated such that it crosses the zero line at least once. This array consists of four small arrays. They are generated using four linear array allocation blocks shown in section A of figure 9. Each block generates a linear array of five elements that makes a straight line with either always positive slope or always negative slope. Concatenating these segments by putting

positive slope segment followed by negative slope segment gives a definite zero crossing. The concatenation block does the process of putting all four segments together and generates an array of twenty elements. Section B in figure 9 shows the multiplication of two consecutive array elements. If the result is negative, both elements are checked for the proximity to zero line by taking their absolute value and deducting it from zero. The index value of point nearest to zero is passed to the section C of figure 9. Formula blocks in section C finds the corresponding value of selected index points and convert them into coordinate form in order to display it on X-Y plot. Thus the whole block diagram works in order to find zero crossing points and display them. Section D in figure 9 shows different types of displays including alphanumeric display for whole array, expanded X-Y plot with all zero crossing points and iconized X-Y plot. Appendix B describes the properties of each block and the formula used for each block. Figure 8 shows the panel view containing the zero crossing points and one of the zero crossing points is shown more clearly in the expanded view in the bottom part of figure 8.

The main view helps understanding the sequence of data flow through the objects that is an implementation of the psuedo code described above. Also, readily available graphical display, alphanumeric display and other components makes the panel view more user-friendly. Embedding a small routine in any large program is possible in VEE. This feature enhances the reusability of any program created in VEE.

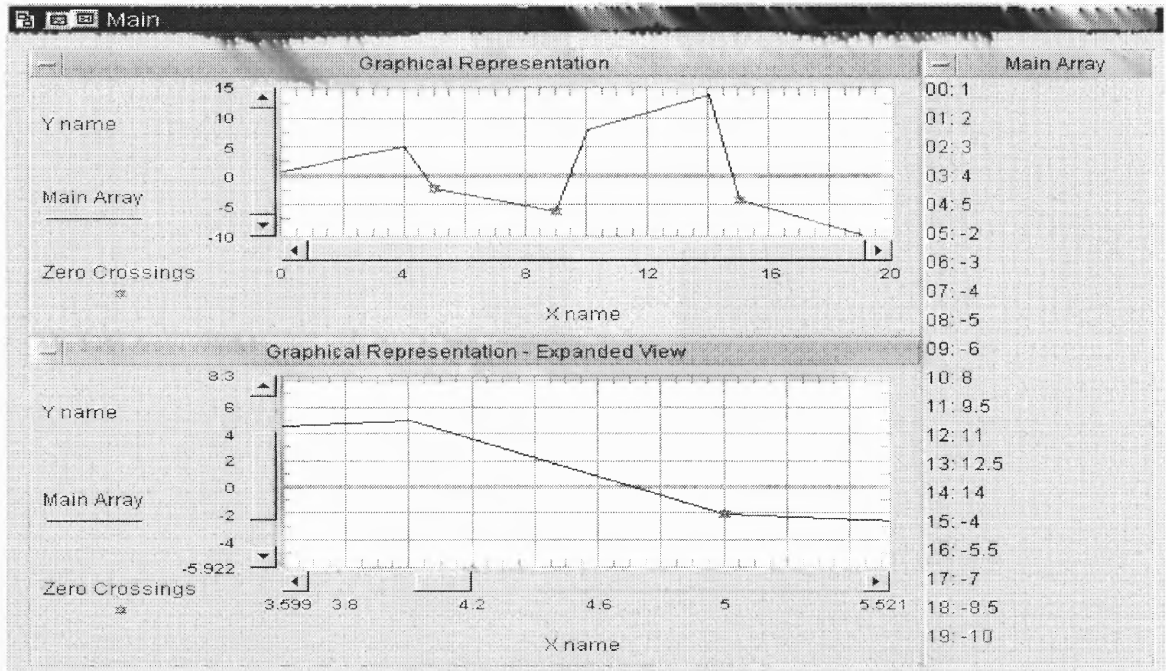


Figure 8: Panel view in VEE.

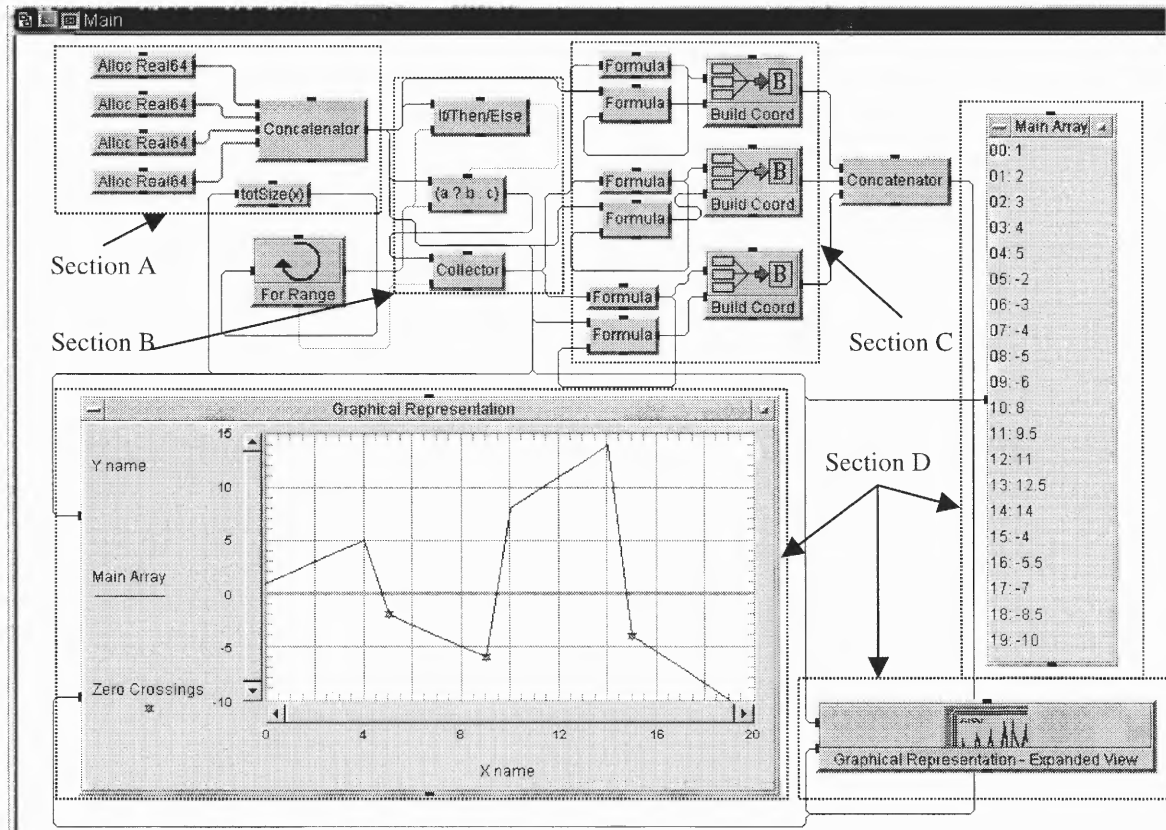


Figure 9: Main view in VEE.

2.2 Acquisition of Data

2.2.1 MIT-BIH Database

In the most emerging field of Medical Engineering, research subjects like Cardiac Arrhythmia Detection, Heart Rate Variability, Electrocardiogram Data Compression, Cardiovascular and Pulmonary Dynamics and Artificial Intelligence-Based Medical Decision Support, etc. are of prime interest. The Massachusetts Institute of Technology (MIT) supplies some valuable resources for such research projects. These resources include databases containing recorded physiological signals and software for analyzing, viewing and creating such recordings. MIT also developed standard software for deriving performance statistics for automated electrocardiogram analyzers required by the current American National Standard (ANSI/AAMI EC38: 1998) for ambulatory electrocardiogram and (ANSI/AAMI EC 57:1998) for testing and respiratory performance results of cardiac rhythm and ST segment measurement algorithms. The MIT-BIH Database (<http://ecg.mit.edu>) is an extended collection of recorded physiological signals.

Various efforts are made in order to prepare such resources for the research community in the biomedical engineering field. This includes work such as developing a very large (~50 GB) database of ICU recordings (the MIMIC Database) of typically 24 to 48 hours in length including 2 to 3 ECG signals, 2 to 4 pressure signals, respiration and extensive clinical data on each subject is being carried out. Development of a long-term ST Database from two-channel 24-hour ECG developments is done by participating in international efforts including the participation of the developers of the European ST-T database.

Software has been developed to read and write digitized signals and annotations using highly portable, flexible and efficient set of database interface functions called “the DB Library”. This software and supporting documentation are freely available from the Internet at (<http://ecg.mit.edu/dbinfo.html>).

From the MIT website <http://ecg.mit.edu/dbinfo.html>, the following items can be downloaded:

- Samples of MIT-BIH Database
- The DB Library
- Software required by ANSI standards mentioned above
- The entire Database software package
- Software called WAVE (Demonstration version) in binary for Linux, Solaris and SunOS
- WVIEW software for MS-Windows users, in binary form
- Documentation including ECG Database programmer’s guide, ECG Database application guide and WAVE user’s guide in postscript and html format
- Updates of earlier versions of the software and Database.

Apart from support of more than 400 users in the last 21 years, organizations like the National Center for Research Resources of the National Institute of Health allows MIT to provide freely almost all data available on CD-ROMs and also helps reduce significantly the cost of CD-ROMs to those who still need them. Currently available databases, software and documentation in the CD-ROM are tabulated at <http://ecg.mit.edu/dbinfo.html#CD-ROMs>.

2.2.2 Method to View and Convert Records

The MIT-BIH database consists of mainly three file formats.

- (1) .hea – Header file
- (2) .atr – Attribute file
- (3) .dat – Data file.

There are also other file formats. For example, .st - sleep stage annotations, .ecg - beat annotations, .qrs - beat annotations, etc. The above listed three main file formats are used to convert each record into text format.

The first thing is to download all sample files available from the page for ECG samples (<http://ecg.mit.edu/dbsamples.html>) and save them to a folder making sure that each set consists of all three file formats with the same file name, e.g., x_100.hea, x_100.atr, x_100.dat.

To convert the available records into the ASCII text format, the following procedure has been used in this project.

1. Copy the rdsamp.exe file, a small program for conversion of the record from its present format into the required ASCII text format, from <http://www.physionet.org/physiotools/binaries/msdos/windows/> into the same folder where you have all sample file sets downloaded.
2. Then run the command `rdsamp -r x_100 -p -v >x_100.txt` to convert the record name x_100 into the ASCII text file format. The output file will be saved in the same folder as x_100.txt.

For more commands on rdsamp application, the general syntax is **rdsamp -r record [options...]** and options can be viewed at manual page for rdsamp

(<http://ecg.mit.edu/dbag/rdsamp-1.htm>). It is required to execute the above command each time to obtain the ASCII text file from every sample record. Likewise, there are other applications also available for various purposes with their manuals and user's guide.

To view these samples in their original form with annotation, the user may download the software related to the appropriate operating system from the software page (<http://ecg.mit.edu/dbinfo.html#DB%20Software%20Package>). The documentation and tutorials for these software packages are available at the documentation page (<http://www.physionet.org/physiotools/wfdb-books.shtml>). The easiest way is to refer to the ECG Database Application Guide at <http://ecg.mit.edu/dbag/dbag.htm> and check their manuals for each command (application) to do various operations on available samples.

2.3 Selection of Samples

The tables below list all the selected samples from the MIT-BIH Database and the QT Database that are considered to validate the algorithms described in this thesis. These samples are carefully chosen such that it includes various events, like motion artifacts, various types of noise signals and noise spikes, PVC events, negative leads, etc. Moreover, these samples are easily available through the Internet. Events in detail for a few samples are available at the MIT-BIH Arrhythmia Database Directory (<http://www.physionet.org/physiobank/database/html/mitdbdir/mitdbdir.htm>).

The first set of samples includes 9 samples from the MIT-BIH Arrhythmia Database (<http://www.physionet.org/physiobank/database/mitdb/>). These samples are chosen specifically to validate the R peak detection algorithm. The results given on the

website of MIT-BIH Arrhythmia Database Directory (<http://www.physionet.org/physiobank/database/html/mitdbdir/mitdbdir.htm>) are used for comparison to validate the analysis process. Each sample in this set is digitized at 360 samples/second and has duration of 30 minutes and 10 seconds. These samples are listed in table 1 with other details.

Table 1: List of samples from MIT-BIH arrhythmia database.

Sr. No	Name of Sample*	Sampling Frequency (Hz)	Age	Sex	No. of Leads	No. of Records in each Lead	No. of R peaks detected by MIT	Length of Sample (min:sec)
1	102	360	84	F	2	650000	2187	30:10
2	105	360	73	F	2	650000	2572	30:10
3	107	360	63	M	2	650000	2137	30:10
4	118	360	69	M	2	650000	2288	30:10
5	119	360	51	F	2	650000	1987	30:10
6	205	360	59	M	2	650000	2656	30:10
7	209	360	62	M	2	650000	3004	30:10
8	214	360	53	M	2	650000	2261	30:10
9	217	360	65	M	2	650000	2208	30:10

The second set of samples is taken from the European ST-T database (<http://www.physionet.org/physiobank/database/edb/>). These samples are chosen such

* Name of sample has been maintained same as the file name of the record in original database.

that all of them have Coronary Artery Disease (CAD) and they are likely to have significant ST-T variation. These characteristics may be useful in measuring significant variance in QT interval. Each signal in this set is sampled at 250 samples/second and is of 15 minutes length. Other details are mentioned in table 2 for this set of samples.

Table 2: Samples from European ST-T database.

Sr. No	Name of Sample*	Sampling Frequency (Hz)	Age	Sex	No. of Leads	No. of Records in each Lead	Length of Sample (min:sec)
1	Sele0104	250	47	M	2	225000	15:00
2	Sele0124	250	58	M	2	225000	15:00
3	Sele0303	250	55	M	2	225000	15:00
4	Sele0406	250	45	M	2	225000	15:00
5	Sele0509	250	34	M	2	225000	15:00
6	Sele0604	250	49	M	2	225000	15:00
7	Sele0606	250	30	M	2	225000	15:00
8	Sele0609	250	46	M	2	225000	15:00

The last set of samples includes all normal patients. These samples are chosen from the Normal Sinus Rhythm database available at (<http://www.physionet.org/physiobank/database/nsrdb/>). This set is particularly useful while doing comparative analysis of the QT interval variability and heart rate variability

* Name of sample has been maintained same as the file name of the record in original database.

between CAD patients and healthy (normal) patients. These samples are digitized at 128 samples/second and other details are given in table 3.

Table 3: Samples from normal sinus rhythm database.

Sr. No	Name of Sample*	Sampling Frequency (Hz)	Age	Sex	No. of Leads	No. of Records in each Lead	Length of Sample (min:sec)
1	16272	128	20	F	2	115200	15:00
2	16420	128	38	F	2	115200	15:00
3	16539	128	35	F	2	115200	15:00
4	16786	128	32	F	2	115200	15:00
5	16795	128	20	F	2	115200	15:00
6	17052	128	45	F	2	115200	15:00
7	18184	128	34	F	2	115200	15:00
8	19093	128	34	M	2	115200	15:00

* Name of sample has been maintained same as the file name of the record in original database.

CHAPTER 3

THE ALGORITHM

The whole algorithm is divided into six different processes:

1. Obtaining the proper inputs
2. Filtering the data
3. Detection of R waves
4. Detection of Q peaks and Q onset
5. Detection of S peaks, T peaks and T wave end
6. Calculating statistical results and construction of the Inter Beat Interval (IBI) and Power Spectrum for QT interval variability and heart rate variability.

This algorithm defines some important variables after every significant step of the analysis process in order to make those values available easily to the next phase of the algorithm.

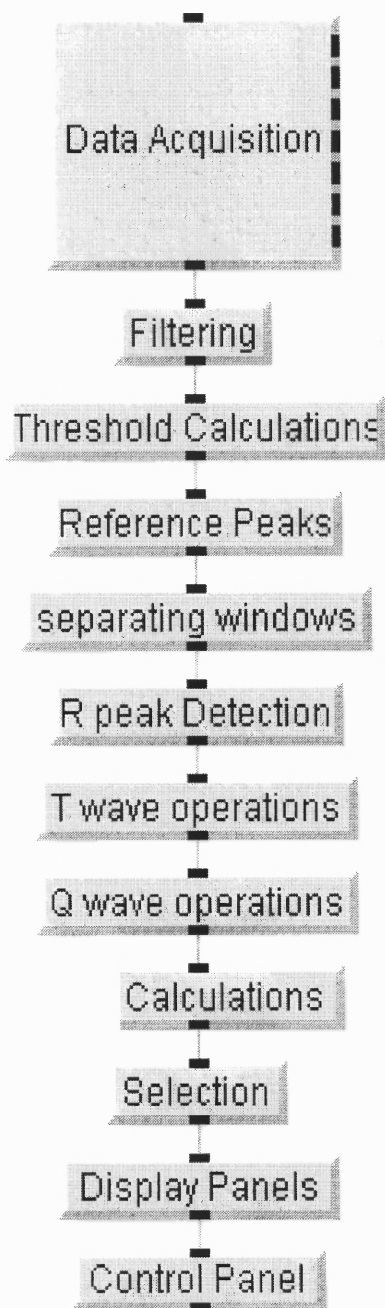


Figure 10: Functional blocks in the program.

3.1 Getting the Proper Inputs

The first step of this algorithm is to read the input data and obtain the sampling frequency from the user. This part of the algorithm gets the input signal, sampling frequency and calculates several variables such as number of records in each lead and number of leads. The module reads the data in ASCII format. The input data must be in a text file with 'tab' delimited, two-dimensional array. The program reads the input array and determines the number of columns which is same as number of leads in the ECG signal. The algorithm works well from any number of leads up to 12. The next step is to prompt for the sampling frequency. The program accepts sampling frequency as integer input between 125 and 1000. The module also checks the length of the sample after getting the sampling frequency value. The ECG record should be of at least two minutes long to obtain maximum resolution for power spectral calculations. If the data is not of required length, then the program terminates automatically. The process also defines various variables, like SF for sampling frequency and NL for number of leads. The screen shot of this routine is available in Appendix A, figure 21.

3.2 Filtering

Filtering is required to avoid errors in the detection of peaks in the ECG signal. There are various kinds of noise signals that can be present in a recorded ECG, viz., power line interference, baseline wander, motion artifact due to electrodes and muscle movements. There can be potential errors in recording caused by even a little carelessness during recording. A special sequence of signal processing algorithm reduces the influence of such noise sources, increases the detection sensitivity, reduces the false detection and

improves the signal-to-noise ratio. The sequence of filtering shown in figure 11 has been implemented to obtain the most suitable filtered signal to process the peak detection analysis accurately.

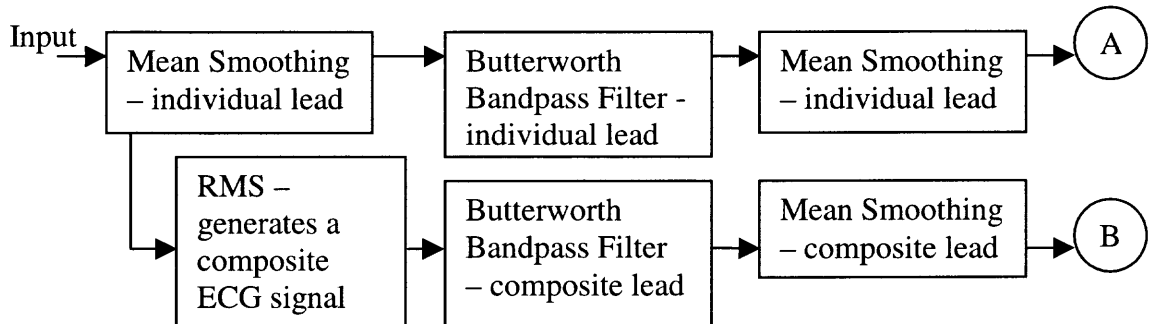


Figure 11: Filtering Process.

The result shown in circle **A** is data from an individual lead after filtering and circle **B** is a composite ECG signal, generated by taking the RMS value of each record for all leads.

Traditionally the lead with most positive R peaks is used to count the R peaks. In this project, the Root Mean Square (RMS) value combining all leads is used. The RMS value provides a good positive signal reducing most of the noise and baseline wandering. The process of taking the RMS value and generating a composite signal for R peak detection eliminates the requirement of manual determination of the best positive lead and makes the analysis more automated.

Mean smoothing was accomplished using a span of 10 points and the bandpass filter has the frequency range of 0.5 Hz to 55 Hz, a second order Butterworth filter. After the filtering process, information about the slope at each point in the waveform is required. The first derivative is taken to obtain information about the slopes and peaks.

All processed signals, such as the filtered original signal and its derivative are stored as variables in order to access them easily in the later part of the algorithm.

The R peaks detected from this composite signal are being considered as fiduciary points for further detection of the Q and T waves. The screen shot of this routine is available in Appendix A, figure 22.

3.3 R Wave Detection

The R wave detection has three subroutines. This detection is done on the composite signal.

1. Adaptive threshold
2. Peak detection from derivative of original signal
3. R peak detection

The QRS complex contains signal components in a relatively wide frequency range from about 2 Hz to 100 Hz with a peak at 10-15 Hz [12]. The R peaks are necessary to be detected accurately for the further detection of the Q and T peaks. In this thesis, the R peak works as a fiduciary point during the detection of the Q and T peaks. The R peak detection is difficult because of physiological variability of QRS complexes and various types of noise that can generate errors in the detection. Sometimes the polarity of the QRS complex and high frequency T waves having similar characteristic as a QRS complex can be a cause of error in the detection. A refractory period of 200 ms following the QRS complex has been set in this project to avoid false detection of T waves or noise spikes.

3.3.1 Adaptive Threshold

This algorithm automatically adjusts the threshold periodically to adapt to QRS morphology and heart rate changes.

Once the original signal (raw data) is filtered and differentiated, this process of adjusting the threshold is implemented. This formula of adaptive threshold is described by P. Laguna *et. al.* [13]. The formula is implemented in the algorithm and can be explained as follows:

Define a threshold at the n th beat as T_n . The threshold is generally some percentage of the maximum value in the predefined time interval of the signal. For example, in this algorithm, sections of 1.5 seconds in duration were used to detect the threshold value for that particular segment. For the first beat, the threshold is 80% of the highest value of that section of signal. For consecutive beats, the threshold is T_{n+1} , which is calculated as,

$$T_{n+1} = 0.8 * T_n + 0.16 * T_{n-1} \quad (1)$$

This formula will set a defined threshold for each 1.5 seconds of the derivative of the original signal and make detection of peaks from the derivative signal easier. The value of the threshold is different for each piece of the signal and the value also depends on the maximum value in that piece. The threshold value will adjust itself even if there is some noise or abnormalities present in the signal. This is called ‘Adaptive Threshold’ algorithm. The screen shot of this routine is also available in Appendix A, figure 23.

3.3.2 Peak Detection from Derivative Signal

Once the threshold has been detected for each section of the derivative signal, the next task is to detect the peaks of the derivative signal because the zero crossing after the peaks of the derivative signal correspond to R peaks in the original signal. The process of detecting peaks can be described as below:

1. Compare each point with corresponding threshold value. If the value is higher than the threshold, save that point in a temporary array.
2. From the array of all points above the threshold, separate the groups of consecutive points above threshold value and store them as temporary variables. If two points are not consecutive, they belong to different QRS complexes and cannot be member of same group. This process will give us number of groups same as number of QRS complexes and each group consisting of few points from one particular QRS complex with value higher than threshold level.
3. Find the maximum value in each group, which will be the tentative peaks.
4. Compare the distance (in terms of ms) between two consecutive tentative peaks. Because two QRS complexes cannot be closer than 200 ms, if the distance between two consecutive tentative peaks is less than 200 ms, ignore the later peak and redefine the array. This concept is called 'Refractory period setting'. Mark those points that have maximum value in each group as peaks.

Results from one of the samples for peak detection is shown in the figure 12. The peaks are marked on the derivative signal.

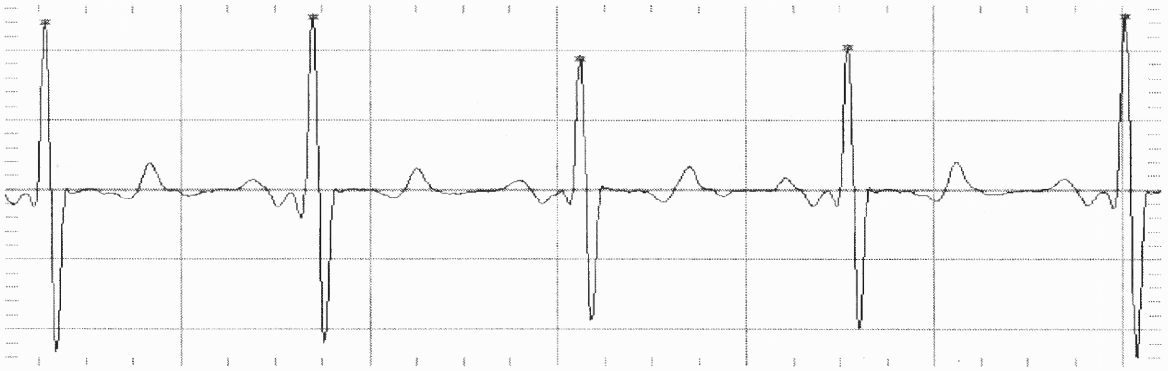


Figure 12: Peak detection using the first derivative of the signal.

3.3.3 Find Zero Crossing Points

The procedure to find the zero crossing point from an array is explained in chapter 2. A similar procedure is used to detect zero crossing points in order to find R peaks. The reason to detect the zero crossing point following each peak detected (peaks from derivative of composite signal) from the previous section is that the zero crossing points (from the derivative of composite signal) are directly associated with R peaks in the original signal. Hence, each peak (peaks from derivative of composite signal) is chosen as a reference point and points following the peak are checked to find a zero crossing. In most cases, unless very severe noise is present, there will be a zero crossing following that particular peak. As most of the noise signal has been removed previously with filtering, there will be a zero crossing following each peak.

These zero crossing points should represent the location for the R peaks in the original data. Thus, by taking this array of zero crossing points, the coordinates of the R peaks can be determined. The graph in figure 13 shows the detected R waves on a composite signal from one of the samples. This routine has a 98% success rate in this project.

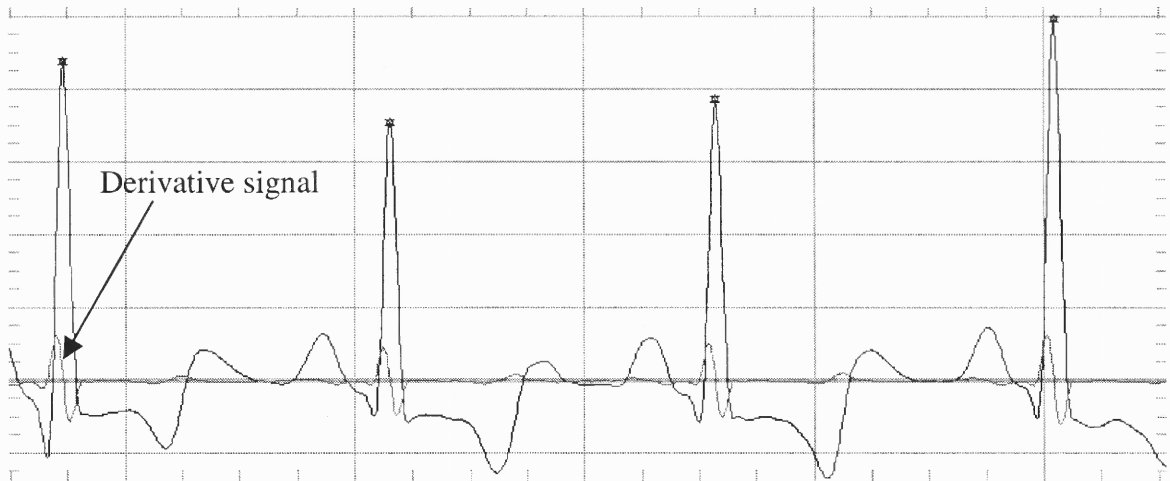


Figure 13: R peaks detection results.

Another sample is shown in figure 14 illustrating successful detection of R peaks even during some abnormalities in the waveform.

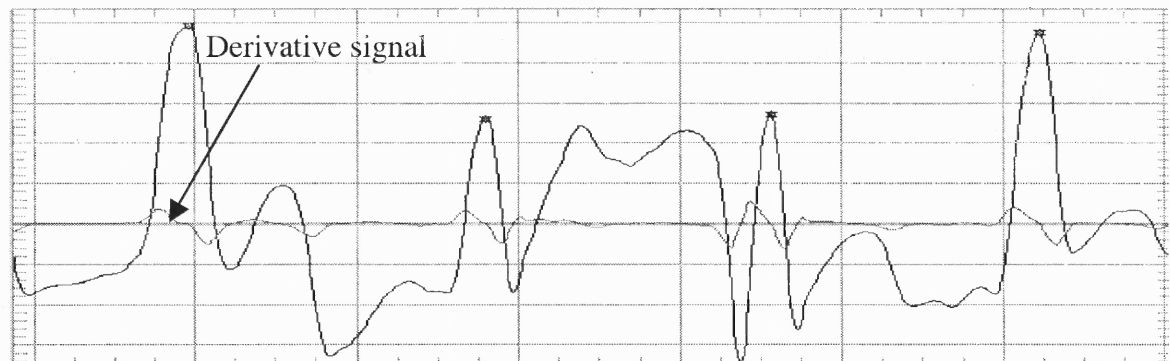


Figure 14: R peaks detected in a noisy piece of signal.

3.4 Q Wave Detection

The Q wave detection process is divided into the following sections:

1. Defining windows
2. Detecting Q wave peak
3. Detecting beginning of Q wave (QRS onset)

3.4.1 Defining Windows

Because the Q peak cannot occur more than 80 ms before the R peak [13], the first window for the Q peak has been defined to 80 ms before the R peak. This window can be easily defined by a taking number of points equal to the $((80 * \text{Sampling-Frequency}) / 1000)$ and converting it to an integer value.

The second window is defined for the span of 40 ms before the end of Q wave window. This window is used to detect the beginning of the QRS complex, also called QRS onset. A similar formula can be used to consider the points for 40 ms as defined in the description of the first window.

3.4.2 Detecting Q Peaks

In the first window of 80 ms of signal before the R peak, there should be a zero crossing preceding the R wave in the derivative of the original signal and as well as a minimum value in the original waveform. This criterion ensures the point as the Q peak. Also, taking the absolute value of samples from the original signal and checking the maximum value and its index can verify the Q peak. If there is no satisfactory detection of the Q wave in this window of 80 ms, the Q wave was marked using the criteria of detecting the minimum value from the windowed signal.

3.4.3 Detecting Q Wave Beginning

The point from where the Q wave begins is detected from the second window of QRS onset. The point nearest to the zero line within this window is said to be the beginning of

QRS complex and marked as the QRS onset point. Due to noise and abnormalities, detection of this point is very difficult. If the point is not detected clearly in the first pass, the QRS onset was marked as the point nearest to the baseline. This helps in maintaining the number of QRS onset points the same as the number of Q peaks and later on in the relevant calculations. This routine is has a 95% success rate in this project.

3.5 T Wave Operations

T wave operations include detection of the T wave peak, T wave end and S wave as an additional point. Again, this process is divided into the following parts:

1. Separating windows
2. Detection of S waves
3. Detection of T peaks
4. Marking end of T waves

3.5.1 Separating Windows

Separating windows in this section is very similar to the previous section. The only difference is the time duration of each window. In this section, we need three separate windows, one for the S wave, one for the T peak and one for the end of the T wave.

The time interval is defined for each window. The first window for the S wave is 150 ms following the R peak. The second window is defined from one of the following:

$$(beginning, end) = (S\ wave, 500\ ms\ from\ R\ peak); \text{ if } RR > 700\ ms \quad (2)$$

$$(beginning, end) = (S\ wave, 0.7 * RR\ ms\ from\ R\ peak); \text{ if } RR < 700\ ms. \quad (3)$$

The formula above shows that the window for the T wave operation is dependent on the previous R-R interval and detection of the S wave. Hence if previous R-R (RR) interval is greater than 700 ms, the window range is from the S wave to 500 ms after the R peak and otherwise it is from the S wave to $0.7*RR$ ms after the R peak. The R peak is considered as a reference to define the end of the window. This ensures the correct window regardless of the accuracy of the S wave detection or prolongation of the S wave. The window size was decreased if the RR decreases in order to avoid false detection of the next P wave. Since the second window can include the T peak as well as the end of the T wave, the algorithm primarily detects only the T peaks.

The window for the end of the T wave is defined from the T peak to the end of second window. This window is physically overlapping the second window but makes the detection of the end of the T wave easier since the T peak is not being considered in this window. Avoiding the T peak in the second window helps avoid confusion in detection of the end of the T wave.

The algorithm is also capable of determining the T wave morphology. The program can detect four different types of T waves, upward-downward T wave, only upward T wave, only downward T wave and downward-upward T wave. The T wave morphology detection is obtained considering slopes at the T peak and the end of T wave. The morphology detection for the T wave is implemented assuming that changes in the T wave morphology might be an indicative of other cardiac abnormalities and future researchers may look into this parameter.

3.5.2 Detection of S Wave

The S wave detection is also implemented as it may help in some future analysis such as ST interval measurements. After the R peak, the window for the S wave has been defined as described in the previous section. Now, the minimum value or the point nearest to the baseline is marked as the S wave. It is also verified using the zero crossing of the derivative of original signal at that point.

3.5.3 Detection of T Peaks

This measurement is very similar to the detection of R peaks. The T wave in most of the ECGs is clear and either positive or negative. The algorithm successfully detects the T wave peak regardless of its polarity.

The window for the T wave was explained in the previous section. In this range of points, the maximum value is the T peak. Since the T wave can be positive or negative, we need to take the absolute value of each point first and redefine each point in the window by taking its absolute value. The absolute value ensures the detection of the correct peak even if the T wave is negative. The detected T wave is also verified by checking the derivative of the signal at that point. The derivative should be a zero crossing point at the point where algorithm determines a T peak. If both criteria are not matching, there is an error message generated and the T peak is considered as a 'doubtful' T peak.

The T wave algorithm also helps to determine the nature of the T wave. It can identify various types of T waves, like, upward, upward-downward, downward and downward-upward T waves. This special feature takes the slope at the T peak and the

end of T wave into consideration to determine the nature of the T wave. The nature of the T wave may be useful in future analysis by comparing morphological changes in the T wave to related physiological or autonomic nervous system changes.

3.5.4 End of T Wave Detection

There is much confusion regarding the end of the T wave. The point where the T wave is assumed to end is very difficult to detect. At the point where T wave ends, the derivative should be zero or close to the baseline. The original signal should also have a zero value or close to the baseline. This criterion ensures the correct detection of the end of the T wave point. This process also works well regardless of the nature of T wave.

The graph shown in figure 15 illustrates the correctly marked S wave, T peak and end of T waves. This subroutine has a 96.7% success rate in this project.

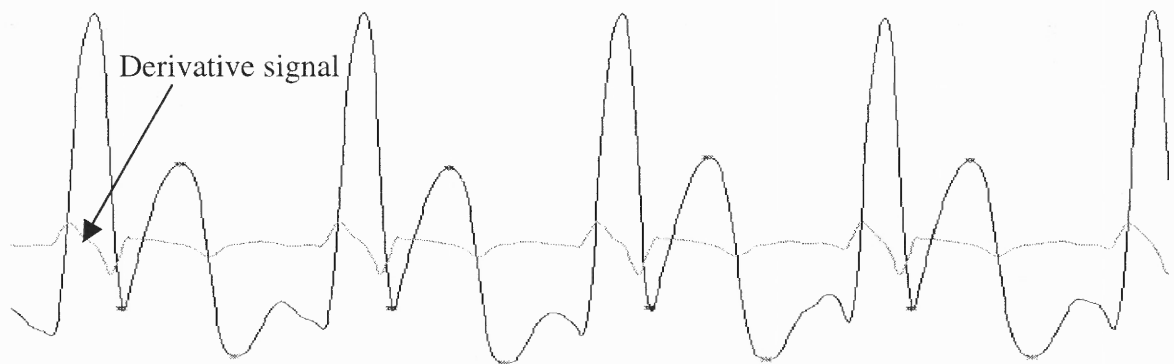


Figure 15: S wave, T peaks and end of T wave results.

3.6 QT Interval Measurements

These measurements are the final stage of the algorithm. The QT interval definition can be stated in several ways. This interval can be from Q wave beginning to the end of the T wave or from the Q peak to the end of the T wave. It can also be from the Q peak to the T

peak or the Q peak to the end of the T wave. The interval is defined from the Q peak to the T peak in this project. Studies showed that defining the end of the QT interval at the maximum of the T wave gave the most precise measurements [6]. Measuring the QT interval from the Q peak to the T peak also reduces the possibility of deviation in the interval calculations due to errors in detection or particular boundary.

The QT interval can have some dependence on the heart rate variability and it is presumed to follow the preceding RR interval [14]. There are formulas to calculate the QTc (QT corrected) that should reduce the influence of the heart rate variability on QT interval variability. Following is the list of formula to calculate QTc [15]:

1. Bazett : $QTc = QT/(RR)^{1/2}$ (3)

2. Fredericia : $QTc = QT/(RR)^{1/3}$ (4)

3. Linear : $QTc = QT + a(1-RR)$; a is a constant obtained form the experiments. (5)

4. Exponential: $QTc = QT - b(e^{-k} - e^{-kRR})$; b, k are constants form the experiments. (6)

In this project, Bazett's formula is used to correct the QT interval as it is the most conventionally used formula. This formula gives QTc (QT corrected) and is defined as, $QTc = QT/(RR)^{1/2}$, where RR is the time interval between the R peak and the previous R peak. This formula is used to reduce the influence due to heart rate variability on QTc, since the measurement of the QT interval variability should be independent of heart rate variability.

The resulting QTc interval calculated by Bazett's formula could still have some dependence on heart rate variability because the calculations and frequency analysis curves are built using the position of the R peaks as reference. To remove the influence of heart rate variability on QT interval variability, a new corrective method is also

introduced in this thesis. It is called QTcc (QT corrected of QTc). Further description about this parameter and construction of the frequency signal using it is given in the next section.

3.7 Obtaining IBI and Power Spectrum

The interbeat interval (IBI) represents the distance between two consecutive R wave peaks in the given ECG signal and spectral analysis is used to provide estimates of sympathetic and parasympathetic influences for the interval variability measurement [16]. The basic purpose of calculating these signals is to observe the amount of influence of the sympathetic and parasympathetic branches of the autonomic nervous system on the QT interval and to compare it with the amount of influence on the hear rate variability.

In order to obtain equidistant IBI samples suitable for frequency analysis and comparison, interpolation is required [16]. In this project, backward interpolation is used to obtain the Interpolated IBI (IIBI). For example, as shown in figure 16, the amplitude represents the RR interval in milliseconds minus the mean at a particular beat and the same value has been interpolated until the previous beat, using a backward step function.

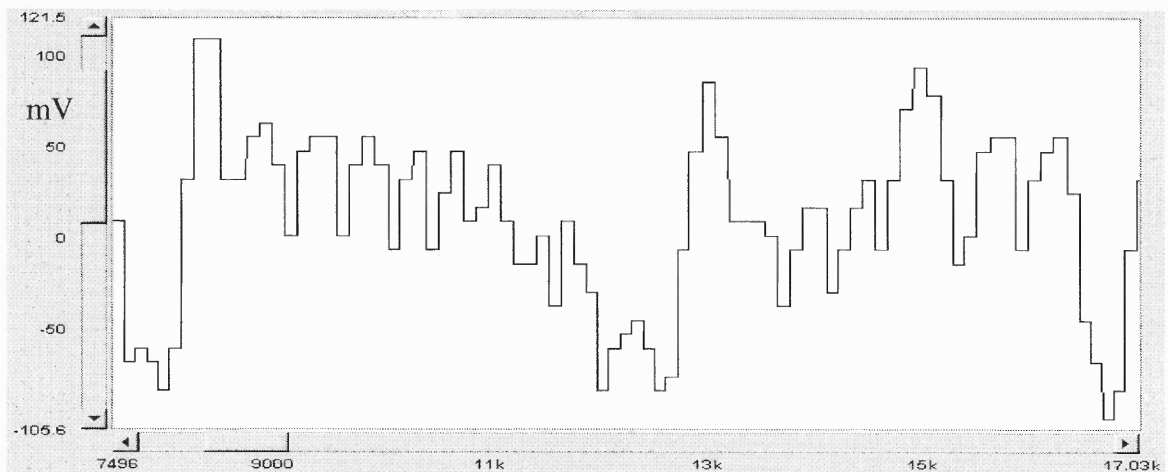


Figure 16: Sample IIBI plot.

Before conducting spectral analysis, the IIBI signal was decimated (by a factor of ten). In this process, every tenth point of the signal is considered for the spectral analysis. The process of decimating the IIBI signal is similar to down sampling. The process of decimation increases the analysis speed and there is no information lost, as the IIBI signal does not contain any frequency component above 6 Hz.

A factor called QTcc (corrected QTc) is considered during the process of construction of the IIBI signal. It is hypothesized in this project that this parameter further eliminates the influence of the heart rate variability on the QT interval. Hence, the IIBI signal for this parameter has been constructed using a constant interval instead using the RR interval. The constant selected in this thesis is 250. Hence, the first beat is plotted at 250; the second beat is at 500 and so on. Power spectral calculations have also been done for QTcc. Results are discussed in the end of this document providing further insight on this hypothesis.

Power spectral analysis of the heart rate variability evaluates activities of the autonomic nervous system noninvasively [17]. The IBI is used as the time domain signal to calculate the power spectrum. Some of the past researchers have associated various peaks from the power spectral analysis with certain physiological parameters [18]. For example, the very low frequency band (0.02 to 0.06 Hz) is associated with vasomotor control and temperature control. The low frequency band (0.06 to 0.15 Hz) correlates baroreceptor-mediated blood pressure control and the high frequency band (0.15 to 0.4 Hz) has been linked with respiration. It has been hypothesized that the low frequency region is representing mixture of both parasympathetic activity and sympathetic activity, whereas the high frequency region corresponds to only parasympathetic activity. One of

the drawbacks of the power spectral analysis of the heart rate variability is that it cannot indicate rapid changes in the heart rate variability over time and joint time-frequency analysis is useful to overcome this drawback [17]. While this thesis does not address this topic, future work can be done using this technique for both heart rate variability and QT variability. Figure 17 shows a sample power spectrum from a healthy patient with clear peaks in very low frequency, low frequency and high frequency regions.

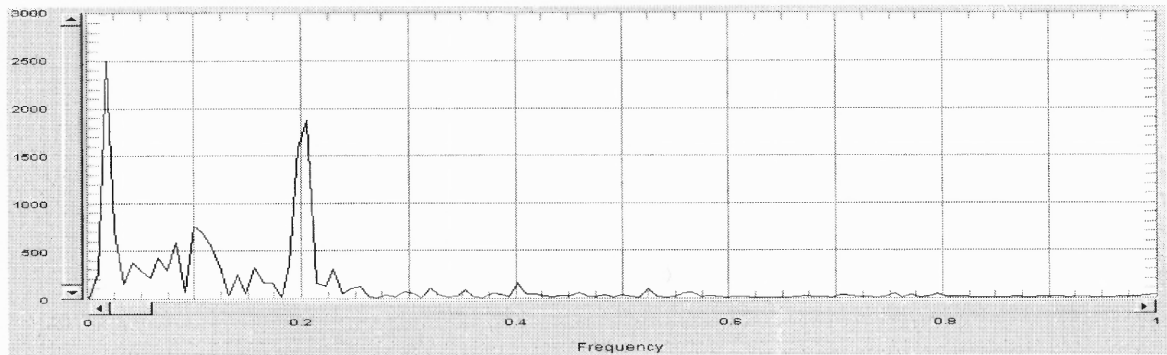


Figure 17: Sample power spectrum from a healthy patient.

Figure 18 and 19 gives a better visual comparison for QTc and QTcc. These diagrams indicate that by calculating power spectrum of QTcc we attenuated one large peak in the high frequency region. This indicates that the measurement and calculation of QTcc parameter reduces the effect of respiration on QT interval variability calculations.

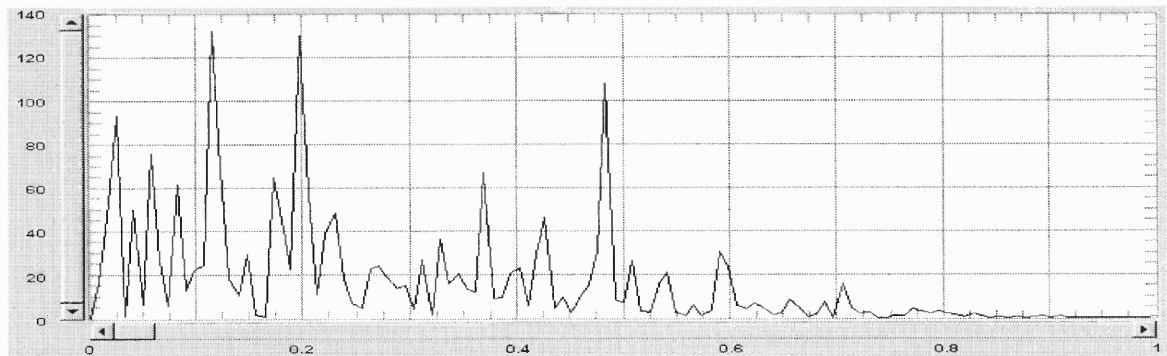


Figure 18: Sample power spectrum for QTc.

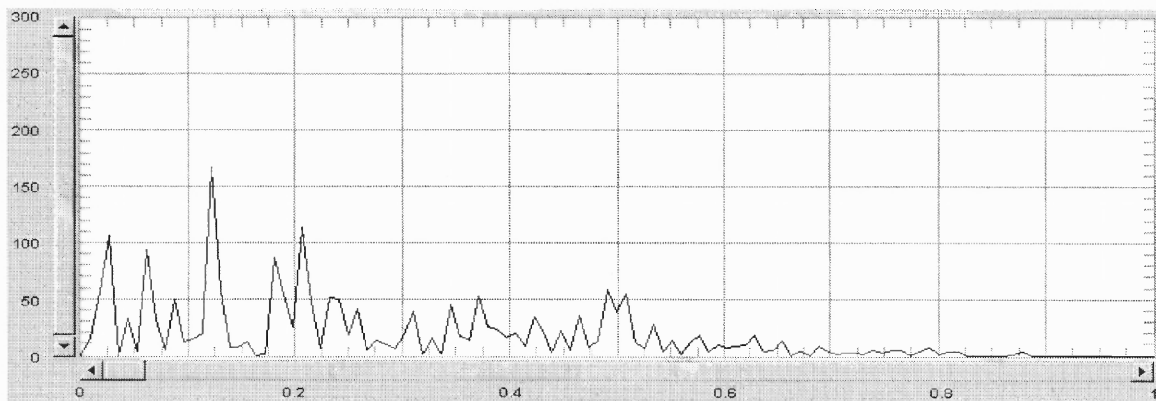


Figure 19: Sample power spectrum for QTcc.

CHAPTER 4

RESULTS AND CONCLUSIONS

As described in Chapter 2, the samples of ECG were selected from the MIT-BIH databases. A total of about 510 minutes in length of data consisting of 56100 heart beats has been analyzed successfully for validation purpose (as shown in Appendix A, table 8).

There are main four parts of the results:

1. R wave validation
2. Q and T wave validation
3. Frequency analysis
4. Comparative analysis

4.1 R Wave Validation

In this research project, an accurate determination of the R peak is an absolutely necessary condition for a reliable Q wave and T wave detection. The information available on MIT's website is used for this validation. The website <http://www.physionet.org/physiobank/database/html/mitdbdir/records.htm> has tabulated information regarding the number of R peaks detected by MIT's algorithm. Comparing the results with MIT's results demonstrate a success ratio of this automated approach. Table 4 shows the comparison between the results of both algorithms' R peak detection:

Table 4: Validation of R wave detection algorithm.

File Name	Sampling Frequency (Hz)	Length (min:sec)	Age (Years)	Sex	Detected R peaks by my algorithm	R peaks by MIT	Success Ratio (%)
102	360	30:10	84	F	2166	2187	99.04
105	360	30:10	73	F	2517	2572	97.86
107	360	30:10	63	M	2136	2137	99.95
118	360	30:10	69	M	2277	2288	99.52
119	360	30:10	51	F	1977	1987	99.50
205	360	30:10	59	M	2622	2656	98.72
209	360	30:10	62	M	2910	3004	96.87
214	360	30:10	53	M	2241	2261	99.12
217	360	30:10	65	M	2144	2208	97.10
Total R peaks					20990	21300	
						Average	98.63

The above table shows a 98.63% success ratio in the selected samples for the R wave detection.

4.2 Q and T Wave Results

For the Q and T wave detections, the author has done manual observation. The results are manually observed using features available in the VEE software for scrolling and

zooming the graphical results. Two minutes of signal from three randomly selected samples has been analyzed. These selected samples are 19093, sele0303 and sele0606. A total of 460 beats were observed manually with the Q peak marked by the algorithm. Only 23 peaks were falsely detected or offset (95% success). This indicates a good success ratio for the algorithm implemented. An example of Q wave results from sample 19093 is shown in figure 20 below:

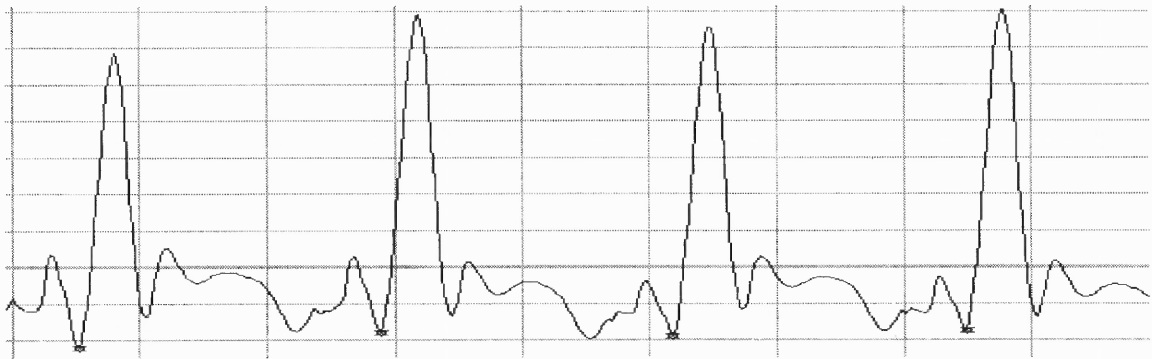


Figure 20: Q wave results.

A similar analysis as used in the Q wave validation was performed for T wave algorithm validation. In the same set of samples for the manual analysis, only 15 T peaks were falsely detected or not accurately detected (96.74% success).

Two types of results are obtained by frequency analysis. As described in the previous chapter, the IIBI plot is obtained for all four parameters, HRV, QT, QTc and QTcc. After calculating the IIBI values, calculations for the Power Spectrum have been done and the spectrum was observed mainly in the 0 to 1 Hz frequency range.

T-test results in table 7 shows that the influence of heart rate variability is not completely removed by calculating QTcc for normal patients.

4.3 Comparative Analysis

To compare HRV with QT interval variability, parameters like area under the low frequency region (LF area), area under the high frequency region (HF area) and ratio of low frequency area and the high frequency area (LF/HF) are compared. A student's t-test for pair of arrays has been done for this analysis. The results are calculated for both groups of patients as shown in the following tables:

Table 5: T-test results comparing each parameter between normal and CAD patients.

	HRV	QT	QTc	QTcc
Std. Dev.	p < 0.0011	p < 0.0015	p < 0.0003	p < 0.0004
HF Area	p < 0.0290	p < 0.2893	p < 0.0233	p < 0.02409
LF Area	p < 0.0270	p < 0.2837	p < 0.0122	p < 0.0075
LF/HF	p < 0.5818	p < 0.5147	p < 0.2848	p < 0.3379

Table 6: T-test results for parameter comparison for CAD patients.

	HRV & QT	HRV & QTc	HRV & QTcc
Std. Dev.	p < 0.0041	p < 0.0014	p < 0.0000005
HF Area	p < 0.3088	p < 0.8745	p < 0.9524
LF Area	p < 0.2172	p < 0.2172	p < 0.9281
LF/HF	p < 0.1769	p < 0.2260	p < 0.2308

Table 7: T-test results for parameter comparison for normal patients.

	HRV & QT	HRV & QTc	HRV & QTcc
Std. Dev.	p < 0.0037	p < 0.00004	p < 0.00003
HF Area	p < 0.0292	p < 0.0363	p < 0.0402
LF Area	p < 0.0270	p < 0.0311	p < 0.03287
LF/HF	p < 0.0007	p < 0.0007	p < 0.0215

The students' t-test is used to check the comparison between parameters. Table 5 compares each parameter, HRV, QT, QTc and QTcc for normal and CAD patients. Table 6 shows the comparison between parameters for CAD patients and table 7 shows the comparison between parameters for normal patients. Parameter comparison has been done by taking HRV & QT, HRV & QTc and HRV & QTCC as pairs for calculations. In table 5, 6 and 7 comparisons have been done for frequency analysis parameters such as LF area, HF area and ratio of LF/HF.

Starting from table 5, the major change in the p value for HF area from HRV to QT indicates that parasympathetic activity is not an influence on heart rate in either normal or CAD patients, but the parasympathetic activity is responsible for major change in QT interval variability for CAD patients. Another observation from table 6 indicates that the parasympathetic nervous system behavior has different mechanism for CAD patients in the case of QT measurements rather than HRV. This makes the dominance of parasympathetic influence on QT for CAD patients very clear. The last observation from table 7 indicates that the parasympathetic and sympathetic activities are not influencing differently for HRV and QT interval variability in the case of normal patients.

The expectation from the parameter comparisons in table 6 or table 7 was that for the values from HRV & QT, HRV & QTc, HRV & QTcc, the statistical significance should change. However, the results indicate no significant difference. This could imply that the effort to remove effect of heart rate change on QT by introducing QTcc is not a better solution, and there is still some influence of heart rate change in QTcc.

Combining all of the above, for CAD patients, the parasympathetic nervous system behaves differently compared to sympathetic nervous system and also compared

to parasympathetic activities in normal patients. Also, the parasympathetic activity influences QT interval variability in a noticeable amount for CAD patients. The activities and influence of the sympathetic nervous system on each index changes in similar fashion as the parasympathetic nervous system influence in both, normal and CAD patient cases. The only difference in the amount of influence of sympathetic activity on each index is low compared to the parasympathetic influence.

4.4 Discussions and Future Work

The analyses of the dynamics of RR or QT time series can only be performed by observing the beat-to-beat variability. There is no 'absolute' unbiased measurement of ventricular repolarization duration due to precision limitations of the tool used. All automatic measurement systems and algorithms produce some error in interval measurement as well. The effort here has been to make the system as much error free as possible using the latest available signal processing software tools. The advantage of this system is that this automatic algorithm rapidly analyses an ECG and is capable of producing a wide range of results. These results can be stored for future work. The performance and reproducibility of the system is comparable between different automatic measurement systems and manual measurement as well. This newly developed system precisely measures the QT interval beat-by-beat over a relatively long period of time with precision of milliseconds. All analyses are performed on the filtered ECG signal and the results are consistent and reliable.

Discussing some of the limitations of the system, the processing time can be reduced using some advanced techniques after significant experience of programming

with VEE. Reducing the number of variables required is one of the key to reduce processing time and virtual memory requirement while analysis. The present system is optimized for 2 lead to 12 lead ECG and sampling frequency range from 125 samples/second to 1000 samples/second. Normally increase in sampling frequency or the length of the ECG signal increases the processing time. Some modifications are necessary to embed the existing system into any real time diagnostic device. Also, the software has wide range of features that makes other calculations of related research very convenient. This whole project serves as a significant step towards the automation of the process and comparative analysis for the two important parameters, the heart rate variability and QT interval for an ECG signal.

The program developed during this thesis is ready for other measurements like QT dispersion and is also ready for analysis of a 12 lead ECG. During the development of the system, the sample data set from the MIT database was also converted into text format and is ready for any kind of future analysis. Future projects can consists of analysis of data with some other hypothesis using the same available program and data set. Also, in the future, researchers may take initiatives to optimize the algorithm, increase the success ratio and reduce the processing time.

APPENDIX A

SCREENSHOTS AND OTHER RESULTS

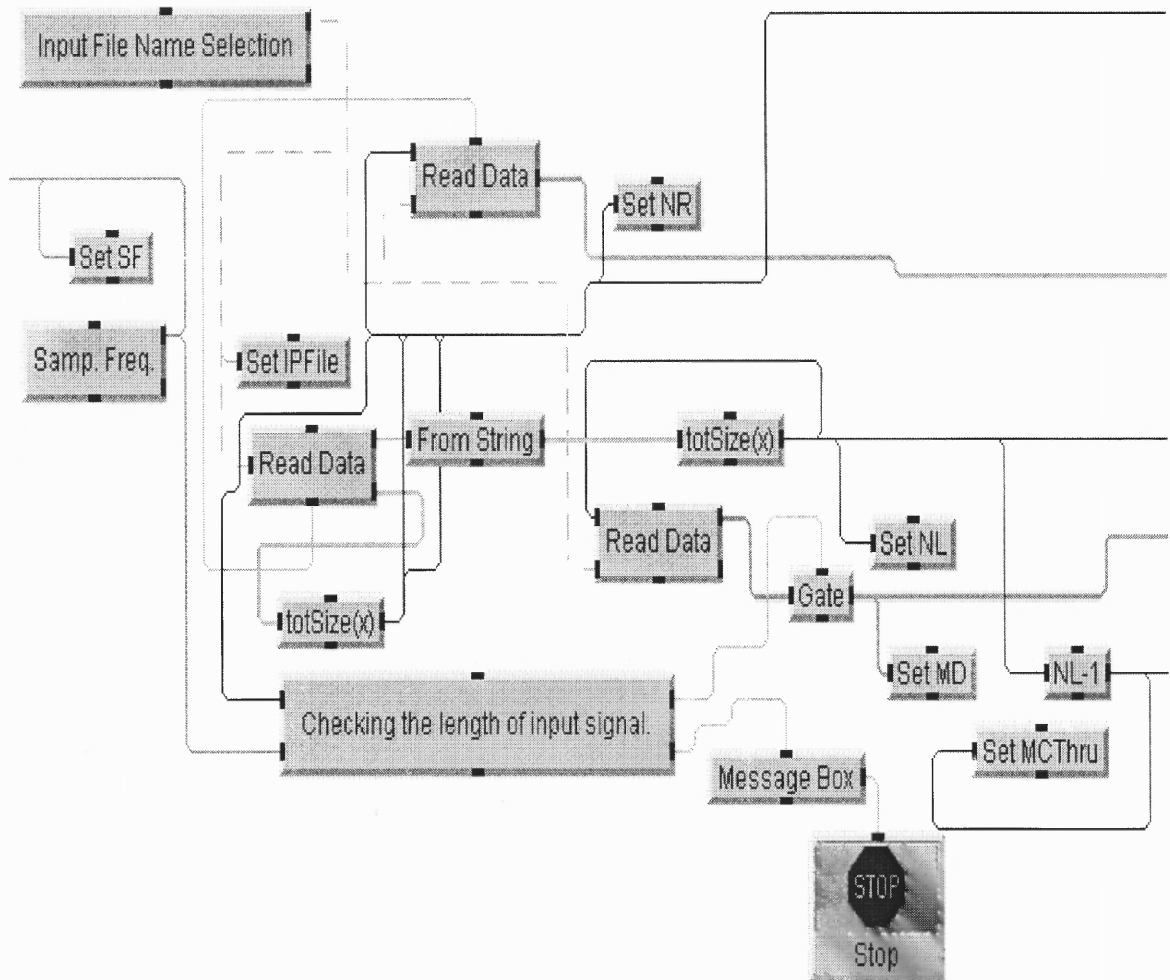


Figure 21: Screenshot of input module.

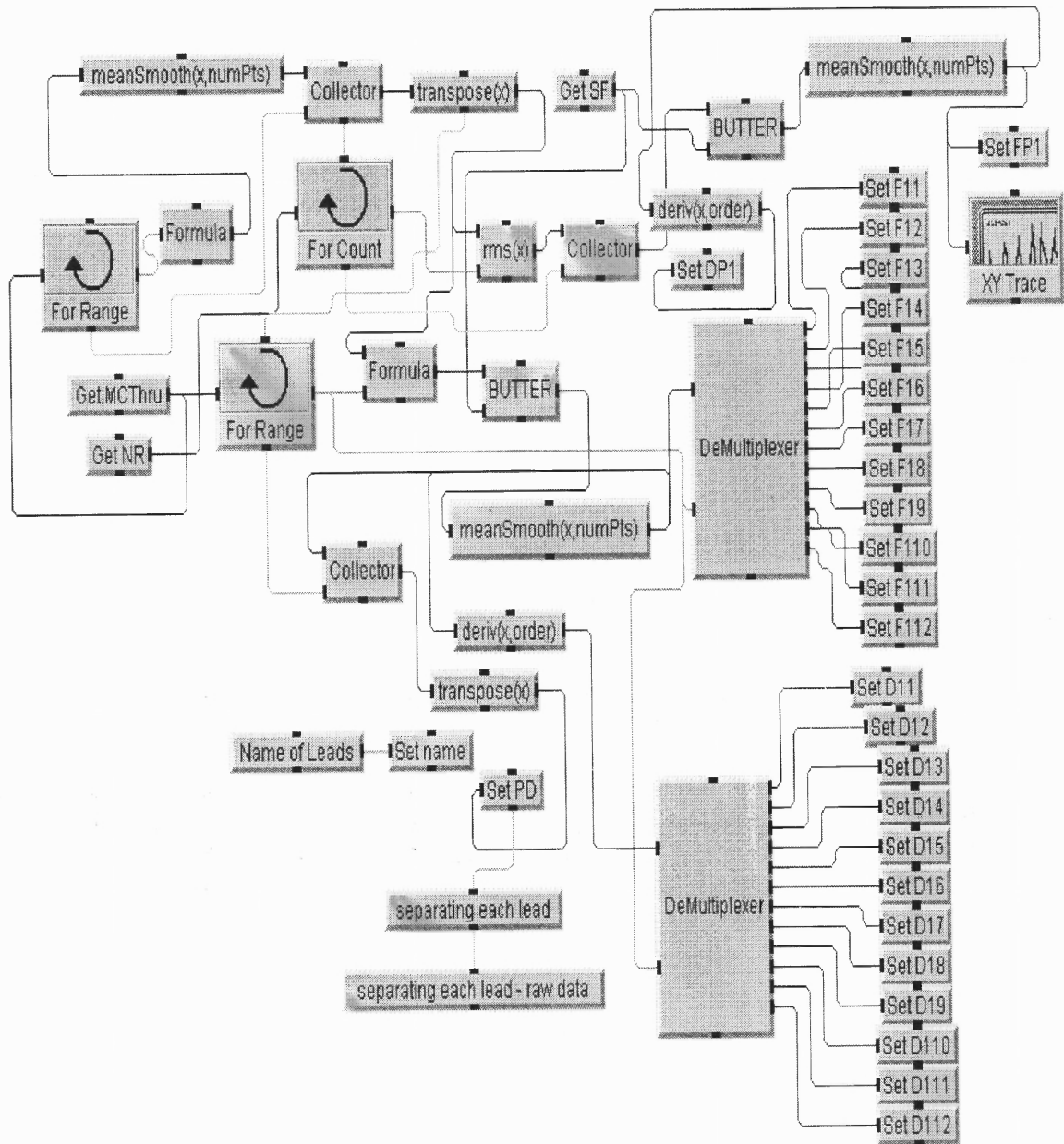


Figure 22: Screenshot of filtering module.

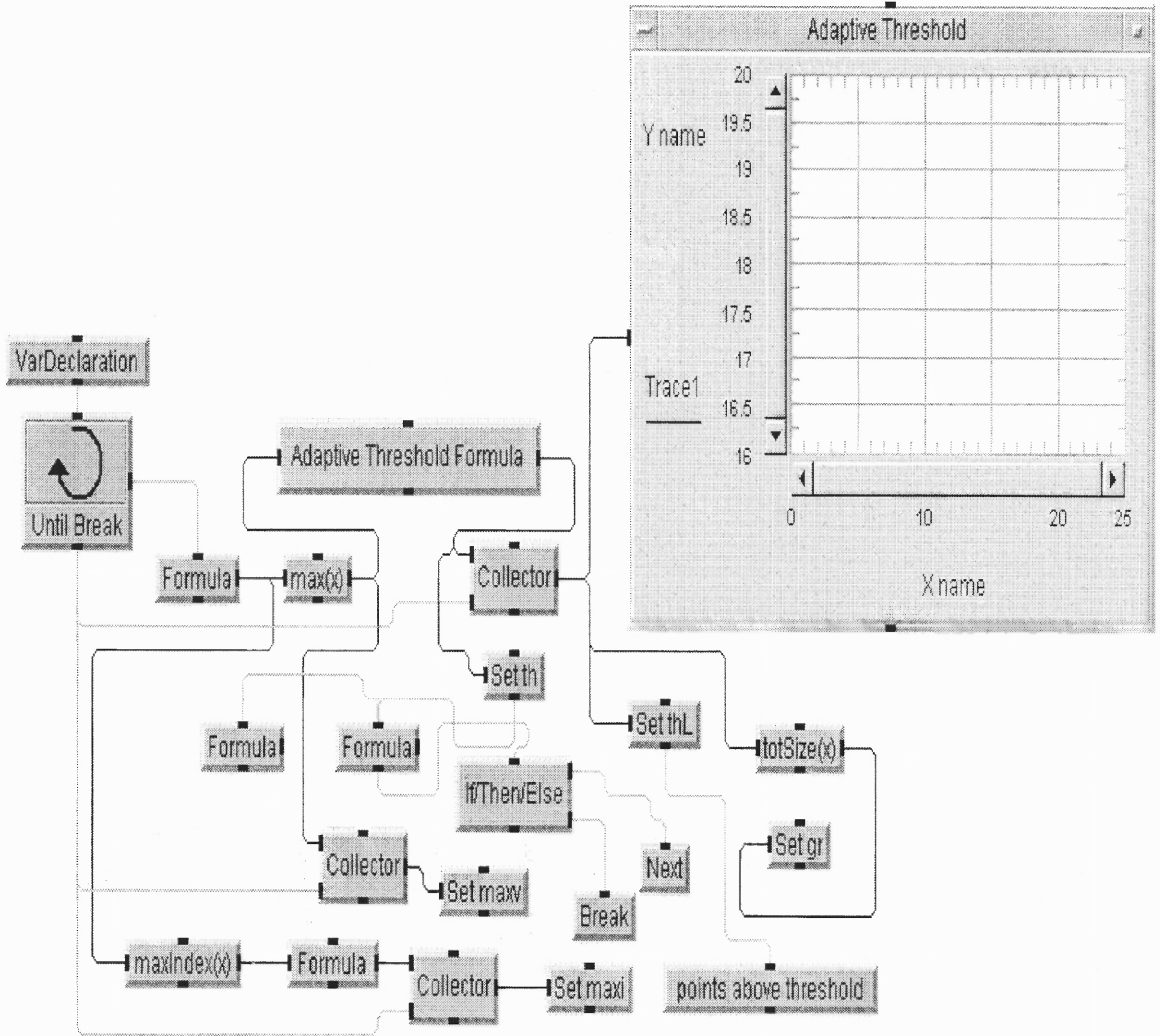


Figure 23: Screenshot of threshold calculation routine.

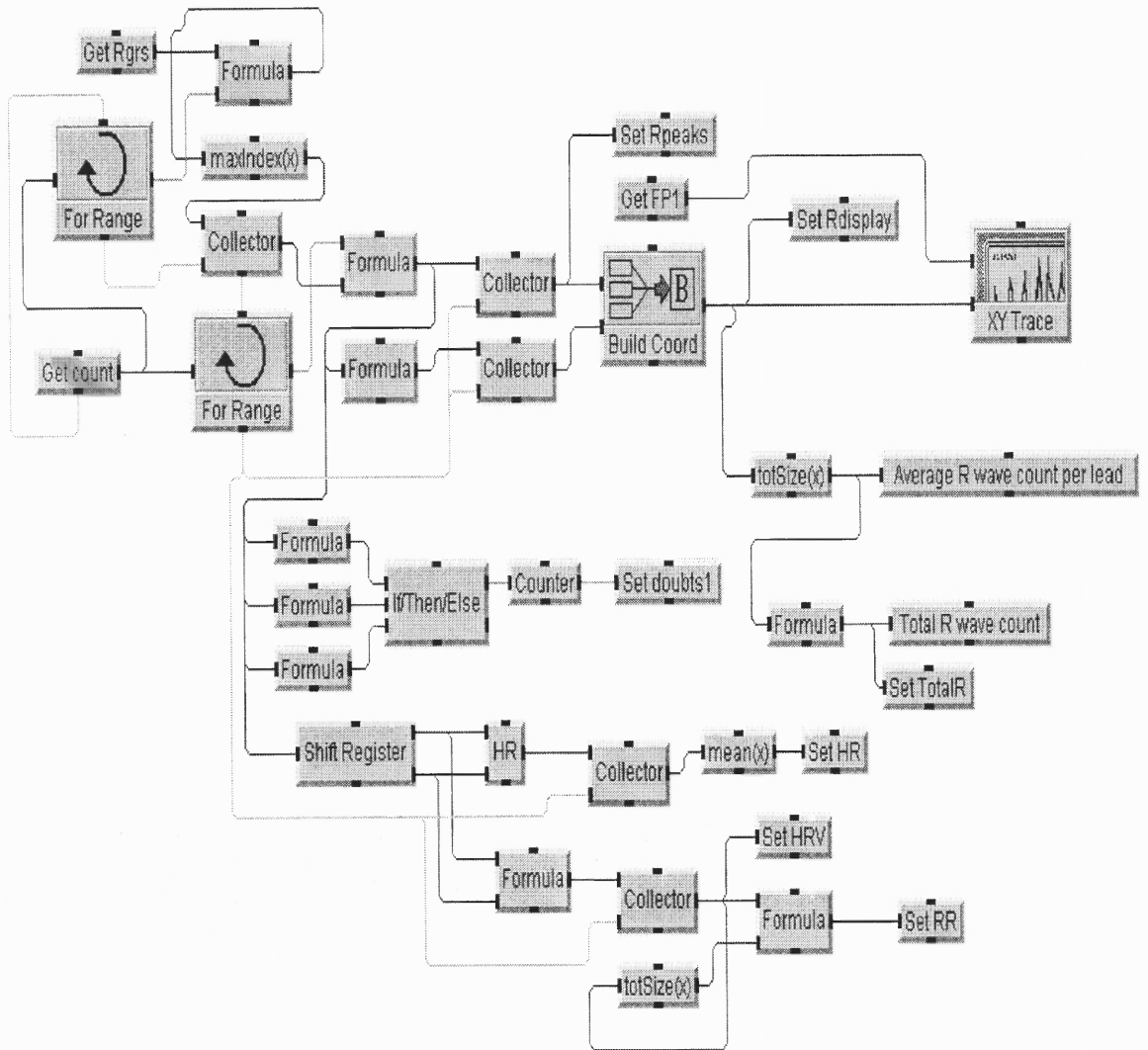


Figure 24: R peak detection routine.

Table 8: Results for number of total beats analyzed.

Sample	No. of R peaks	HR
102	2166	72.2
105	2517	83.9
107	2136	72.2
118	2277	75.9
119	1977	65.9
205	2622	87.4
209	2910	97
214	2241	74.4
217	2144	71.5
Sele0104	1608	53.8
Sele0124	2242	74.9
Sele0303	2088	69.9
Sele0406	1918	64.2
Sele0509	2058	70
Sele0604	2062	70.4
Sele0606	2880	96.8
Sele0609	2252	75.7
16272	2138	77.1
16420	2566	88.8
16539	2492	87.9
16786	2162	74.2
16795	2052	74.1
17052	2372	83.6
18184	2228	87.1
19093	1992	69.3

APPENDIX B

AN EXAMPLE OF PROGRAM DOCUMENTATION

VEE revision: 6.0
Execution Mode: VEE 6
Convert Infinity on Binary Read: no

I/O Configuration

Embedded Configuration

GPIB0

dmm(@(NOT LIVE))
 Panel Driver: hp34401a.cid
 Timeout (sec): 1.000000
 Byte ordering: MSB
dvm(@(NOT LIVE))
 Panel Driver: hp3478a.cid
 Timeout (sec): 5.000000
 Byte ordering: MSB
fgen(@(NOT LIVE))
 Panel Driver: hp3325b.cid
 Timeout (sec): 5.000000
 Byte ordering: MSB

M: Main

Device Type : Main
Context is secured : off
Trig mode : Degrees
Popup Panel Title Text : Untitled
Show Popup Panel Title : on
Show Popup Panel Border : on
Popup Moveable : on
Popup Panel Title Text Color : Object Title Text
Popup Panel Title Background Color : Object Title
Popup Panel Title Text Font : Object Title Text
Delete Globals at Prerun : on

M.0: Main/Alloc Real64

Device Type : Allocate Array
Output pin 1 : Array

M.1: Main/Alloc Real64

Device Type : Allocate Array
Output pin 1 : Array

M.2: Main/Alloc Real64

Device Type : Allocate Array
 Output pin 1 : Array

M.3: Main/Alloc Real64

Device Type : Allocate Array
 Output pin 1 : Array

M.4: Main/Concatenator

Device Type : Concatenator
 Input pin 1 : A (Any, Any)
 Input pin 2 : B (Any, Any)
 Input pin 3 : C (Any, Any)
 Input pin 4 : D (Any, Any)
 Output pin 1 : Array

M.5: Main/totSize(x)

Device Type : Formula
 Input pin 1 : x (Any, Any)
 Output pin 1 : Result
 Formula : totSize(x)-1

M.6: Main/If/Then/Else

Device Type : If/Then/Else
 Input pin 1 : A (Any, Any)
 Input pin 2 : B (Any, Any)
 Output pin 1 : Then
 Output pin 2 : Else
 If/Else cases : $A[B]*A[B-1] \leq 0$

M.7: Main/For Range

Device Type : For Range
 Input pin 1 : Thru (Real64, Scalar)
 Output pin 1 : Data
 From Value : 1
 Thru Value : 19
 Step Value : 1

M.8: Main/Collector

Device Type : Collector
 Input pin 1 : Data (Any, Any)
 Input pin 2 : XEQ (Any, Any)
 Output pin 1 : Array
 Clear At Prerun : on
 Clear at Activate : on
 Output shape 1d : off

M.9: Main/(a ? b : c)

Device Type : Formula
 Input pin 1 : a (Any, Any)
 Input pin 2 : b (Any, Any)
 Output pin 1 : Result
 Formula : ((abs(a[b]))<(abs(a[b-1])) ? b : b-1)

M.10: Main/Graphical Representation

Device Type : Y Plot
 Input pin 1 : Main Array (Any, Any)
 Input pin 2 : Zero Crossings (Any, Any)
 Clear At Prerun : on
 Clear at Activate : on

M.11: Main/Concatenator

Device Type : Concatenator
 Input pin 1 : A (Any, Any)
 Input pin 2 : B (Any, Any)
 Input pin 3 : C (Any, Any)
 Output pin 1 : Array

M.12: Main/Build Coord

Device Type : Build Coord
 Input pin 1 : X Data (Real64, Any)
 Input pin 2 : Y Data (Real64, Any)
 Output pin 1 : Coord

M.13: Main/Build Coord

Device Type : Build Coord
 Input pin 1 : X Data (Real64, Any)
 Input pin 2 : Y Data (Real64, Any)
 Output pin 1 : Coord

M.14: Main/Build Coord

Device Type : Build Coord
 Input pin 1 : X Data (Real64, Any)
 Input pin 2 : Y Data (Real64, Any)
 Output pin 1 : Coord

M.15: Main/Formula

Device Type : Formula
 Input pin 1 : A (Any, Any)
 Input pin 2 : B (Any, Any)
 Output pin 1 : Result
 Formula : A[B]

M.16: Main/Formula

Device Type : Formula
 Input pin 1 : A (Any, Any)
 Input pin 2 : B (Any, Any)
 Output pin 1 : Result
 Formula : A[B]

M.17: Main/Formula

Device Type : Formula
 Input pin 1 : A (Any, Any)
 Input pin 2 : B (Any, Any)
 Output pin 1 : Result
 Formula : A[B]

M.18: Main/Formula

Device Type : Formula
 Input pin 1 : A (Any, Any)
 Output pin 1 : Result
 Formula : A[2]

M.19: Main/Formula

Device Type : Formula
 Input pin 1 : A (Any, Any)
 Output pin 1 : Result
 Formula : A[1]

M.20: Main/Formula

Device Type : Formula
 Input pin 1 : A (Any, Any)
 Output pin 1 : Result
 Formula : A[0]

M.21: Main/Main Array

Device Type : AlphaNumeric
 Input pin 1 : Data (Any, Any)
 Clear At Prerun : on
 Clear at Activate : on
 Indices Enabled : on

REFERENCES

1. http://www.merck.com/pubs/mmanual_home/home.html, 12/12/00 12:33 PM.
2. L. Cromwell, F. Weibell, E. Pfeiffer. *Biomedical Instrumentation and Measurements*, Prentice-Hall, 1996.
3. http://medstat.med.utah.edu/kw/ecg/ecg_outline/index.html, 12/12/00 12:33 PM.
4. A. Alagra, H. Le Brun, C. Zeelenberg, "An algorithm for computer measurement of QT intervals in the 24-hour ECG," IEEE 1987, 117-119.
5. P. Caminal, A. Blasi, M. Vallverdu, X. Vinolas, R. Jane, P. Laguna, M. V. Pitzalis, P. Rizzon, W. Zareba, A. Bayes, "New algorithm for QT dispersion analysis in XYZ-Lead Holter ECG: performance and applications," Computers in Cardiology, IEEE, 1998, 709-712.
6. P. E. Tikkanen, L. C. Sellin, H. O. Kinnunen, H. V. Huikuri, "Using simulated noise to define optimal QT intervals for computer analysis of ambulatory ECG," Medical Engineering & Physics 21, 1999, 15-25.
7. J. S. Sahambi, S. N. Tandon, R. K. P. Bhatt, "An automated approach to beat-by-beat QT interval analysis," IEEE Engineering in Medicine and Biology, May/June 2000, 97-100.
8. M. Malik, et al., "Heart Rate Variability: Standards of Measurement, Physiological Interpretation and clinical use – Special Report," Circulation, 1996, 1043-1065.
9. Hon E. H., Lee S. T., "Electronics evaluations of the fetal heart rate patterns preceding fetal death: further observations," Am J obstet Gynecol, 1965, 814-826.
10. Wolf M. M., Varigos G. A., Hunt D, Sloman J. G., "Sinus arrhythmia in acute myocardial infarction," Med J Aust., 1978, 52-53.
11. Akselrod S, Gordon D, Ubel F. A., Shannon D. C. Barger A. C., Cohen R. J., "Power Spectrum analysis of heart rate fluctuation: a quantitative probe of beat-to-beat cardiovascular control," Science, 1981, 220-222.
12. A. Ruha, S. Sallinen, S. Nissila, "A real-time microprocessor QRS detector system with a 1-ms timing accuracy for measurement of ambulatory HRV," IEEE Transaction on Biomedical Engineering, Vol. 44, No. 3, March 1997, 159-167.
13. P. Laguna, N.V. Thakor, P. Caminal, R. Jane, Hyung-Ro-Yoon, A. Bayes de Luna, V. Marti, Josep Guindo, "New algorithm for QT interval analysis in 24-hour Holter ECG: performance and applications," Medical & Biological Engineering & Computing, January 1990, 28, 67-73.

14. D. G. Segal, M. M. Radai, Y. Sivan, S. Abboud, "*Real-time PC-Based system for dynamic beat-to-beat QT-RR analysis,*" Computers and Biomedical Research 32, 1999. 336-354.
15. F. Badilini, P. Mainson-Blanche, R. Spaulding, M. Palma, P. Coumel, "*Analysis of QT interval during passive tilt test: Comparison of different correction formula,*" Computers in Cardiology, 1998, Vol. 25, 713-716.
16. S. Fernando, "*Autonomic nervous system evaluation using time-frequency analysis,*" NJIT, MS Thesis, October 1994.
17. R. Saliba, "*Bilinear time-frequency representations of heart rate variability and respiration during stress,*" NJIT, Ph. D. Dissertation, January 1997.
18. Chess G. F., Tam R. M. K. and F. R. Calresu. "*Influence of cardiac neural inputs on rhythmic variations of heart period in the cat,*" Amer. J. Physiol., Vol. 228, 1975, 775-780.